

# Synthesis of inorganic nanomaterials

C. N. R. Rao,<sup>\*a,b</sup> S. R. C. Vivekchand,<sup>a</sup> Kanishka Biswas<sup>a,b</sup> and A. Govindaraj<sup>a,b</sup>

Received 1st June 2007, Accepted 9th July 2007

First published as an Advance Article on the web 6th August 2007

DOI: 10.1039/b708342d

Synthesis forms a vital aspect of the science of nanomaterials. In this context, chemical methods have proved to be more effective and versatile than physical methods and have therefore, been employed widely to synthesize a variety of nanomaterials, including zero-dimensional nanocrystals, one-dimensional nanowires and nanotubes as well as two-dimensional nanofilms and nanowalls. Chemical synthesis of inorganic nanomaterials has been pursued vigorously in the last few years and in this article we provide a perspective on the present status of the subject. The article includes a discussion of nanocrystals and nanowires of metals, oxides, chalcogenides and pnictides. In addition, inorganic nanotubes and nanowalls have been reviewed. Some aspects of core-shell particles, oriented attachment and the use of liquid-liquid interfaces are also presented.

## 1. Introduction

Nanoscience involves a study of materials where at least one of the dimensions is in the 1–100 nm range. Properties of such materials are strongly dependant on their size and shape. Nanomaterials include zero-dimensional nanocrystals, one-dimensional nanowires and nanotubes and two-dimensional nanofilms and nanowalls. Synthesis forms an essential component of nanoscience and nanotechnology. While nanomaterials have been generated by physical methods such as laser ablation, arc-discharge and evaporation, chemical methods have proved to be more effective, as they provide better control as well as enable different sizes, shapes and functionalization. Chemical synthesis of nanomaterials has been reviewed by a few authors,<sup>1–6</sup> but innumerable improvements and better methods are being reported continually in the last few years. In accomplishing the synthesis and manipulation of the nanomaterials, a variety of reagents and strategies have been employed besides a wide spectrum of reaction conditions. In view of the intense research activity related to nanomaterials synthesis, we have prepared this perspective to present recent developments and new directions in this area. In doing so, we have dealt with all classes of inorganic nanomaterials. In writing such an article, it has been difficult to do justice to the vast number of valuable contributions which have appeared in the literature in last the two to three years. We had to be necessarily succinct and restrict ourselves mainly to highlighting recent results.

## 2. Nanocrystals

Nanocrystals are zero-dimensional particles and can be prepared by several chemical methods, typical of them being reduction of salts, solvothermal synthesis and the decomposition of molecular precursors, of which the first is the most common method used

in the case of metal nanocrystals. Metal oxide nanocrystals are generally prepared by the decomposition of precursor compounds such as metal acetates, acetylacetonates and cupferronates in appropriate solvents, often under solvothermal conditions. Metal chalcogenide or pnictide nanocrystals are obtained by the reaction of metal salts with a chalcogen or pnictogen source or the decomposition of single source precursors under solvothermal or thermolysis conditions. Addition of suitable capping agents such as long-chain alkane thiols, alkyl amines and trioctylphosphine oxide (TOPO) during the synthesis of nanocrystals enables the control of size and shape. Monodisperse nanocrystals are obtained by post-synthesis size-selective precipitation.

### 2.1 Metals

Reduction of metal salts in the presence of suitable capping agents such as polyvinylpyrrolidone (PVP) is the common method to generate metal nanocrystals. Solvothermal and other reaction conditions are employed for the synthesis, to exercise control over their size and shape of the nanocrystals.<sup>1,2,7</sup> Furthermore, the sealed reaction conditions and presence of organic reagents reduce the possibility of atmospheric oxidation of the nanocrystals. The popular citrate route to colloidal Au, first described by Hauser and Lynn,<sup>8</sup> involves the addition of chloroauric acid to a boiling solution of sodium citrate.<sup>9</sup> The average diameter of the nanocrystals can be varied over the 10–100 nm range by varying the concentration of reactants. Au nanocrystals with diameters between 1 and 2 nm are obtained by the reduction of HAuCl<sub>4</sub> with tetrakis(hydroxymethyl)phosphonium chloride (THPC) which also acts as a capping agent.<sup>10</sup> Following the early work of Brust and co-workers,<sup>11</sup> the general practice employed to obtain organic-capped metal nanocrystals is to use a bi-phasic mixture of an organic solvent and the aqueous solution of the metal salt in the presence of a phase-transfer reagent. The metal ion is transferred across the organic-water interface by the phase transfer reagent and subsequently reduced to yield sols of metal nanocrystals. Metal nanocrystals in the aqueous phase can also be transferred to a nonaqueous medium by using alkane thiols to obtain organosols.<sup>12,13</sup> This method has been used to thiolize

<sup>a</sup>Chemistry and Physics of Materials Unit, DST unit on nanoscience and CSIR Centre of Excellence in Chemistry, Jawaharlal Nehru Centre for Advanced Scientific Research, Jakkur P. O., Bangalore, 560064, India. E-mail: cnrrao@jncasr.ac.in; Fax: +91 80 22082760

<sup>b</sup>Solid State and Structural Chemistry Unit, Indian Institute of Science, Bangalore, 560012, India

C. N. R. Rao obtained his PhD degree from Purdue University and DSc degree from the University of Mysore. He is the Linus Pauling Research Professor at the Jawaharlal Nehru Centre for Advanced Scientific Research and Honorary Professor at the Indian Institute of Science (both at Bangalore). His research interests are in the chemistry of materials. He has authored nearly 1000 research papers and edited or written 30 books in materials chemistry. A member of several academies including the Royal Society and the US National Academy of Sciences, he is the recipient of the Einstein Gold Medal of UNESCO, Hughes Medal of the Royal Society, and the Somiya Award of the International Union of Materials Research Societies (IUMRS). In 2005, he received the Dan David Prize for materials research from Israel and the first India Science Prize.

S. R. C. Vivekchand received his BSc degree from The American College, Madurai in 2001. He is a student of the integrated PhD programme of Jawaharlal Nehru Centre for Advanced Scientific Research, Bangalore and received his MS degree in 2004. He has worked primarily on material chemistry aspects of one-dimensional nanomaterials.

Kanishka Biswas received his BSc degree from Jadavpur University, Kolkata in 2003. He is a student of the integrated PhD programme of Indian Institute of Science, Bangalore and received his MS degree in 2006. He has worked primarily on the synthesis and characterization of inorganic nanomaterials.

A. Govindaraj obtained his PhD degree from University of Mysore and is a Senior Scientific Officer at the Indian Institute of Science, and Honorary Faculty Fellow at the Jawaharlal Nehru Centre for Advanced Scientific Research. He works on different types of nanomaterials. He has authored more than 100 research papers and co-authored a book on nanotubes and nanowires.



C. N. R. Rao



S. R. C. Vivekchand



Kanishka Biswas



A. Govindaraj

Pd nanocrystals with magic numbers of atoms.<sup>14,15</sup> A method to produce gold nanocrystals free from surfactants would be to reduce  $\text{HAuCl}_4$  by sodium naphthalenide in diglyme.<sup>16</sup>

Liz-Marzán and co-workers<sup>17</sup> have prepared nanoscale Ag nanocrystals by using dimethylformamide as both a stabilizing agent and a capping agent. By using tetrabutylammonium borohydride or its mixture with hydrazine, Jana and Peng<sup>18</sup> obtained monodisperse nanocrystals of Au, Cu, Ag, and Pt. In this method,  $\text{AuCl}_3$ ,  $\text{Ag}(\text{CH}_3\text{COO})$ ,  $\text{Cu}(\text{CH}_3\text{COO})_2$ , and  $\text{PtCl}_4$  were dispersed in toluene with the aid of long-chain quaternary ammonium salts and reduced with tetrabutylammonium borohydride which is toluene-soluble. The reaction can be scaled up to produce gram quantities of nanocrystals. Mirkin and co-workers<sup>19–21</sup> have devised two synthetic routes for nanoprisms of Ag. In the first method, Ag nanoprisms (Fig. 1a) are produced by irradiating a mixture of sodium citrate and bis(*p*-sulfonatophenyl) phenylphosphine dihydrate dipotassium capped Ag nanocrystals with a fluorescent lamp. In the second method,  $\text{AgNO}_3$  is reduced with a mixture of borohydride and hydrogen peroxide.<sup>21</sup> The latter method has been extended to synthesize branched nanocrystals of Au of the type shown in Fig. 1b and 1c.<sup>22,23</sup>

The shape and colour of Au nanoparticles can be altered by NAD(P)H-mediated growth in the presence of ascorbic acid.<sup>24</sup>

The method yields dipods, tripods and tetrapods (nanocrystals with 2, 3 and 4 arms respectively, the one with 4 arms generally being tetrahedral). Icosahedral Au nanocrystals are obtained by the reaction of  $\text{HAuCl}_4$  with PVP in aqueous media.<sup>25</sup> Right-bipyramid (75–150 nm in edge length) nanocrystals of Ag (Fig. 2) have been prepared by the addition of NaBr during the polyol reduction of  $\text{AgNO}_3$  in the presence of PVP.<sup>26</sup> Cu nanoparticles of pyramidal shape have been made by an electrochemical procedure.<sup>27</sup>

Nanoparticles of Rh and Ir have been prepared by the reduction of the appropriate compounds in the ionic liquid, 1-*n*-butyl-3-methylimidazoliumhexafluorophosphate, in the presence of hydrogen.<sup>28</sup> Synthesis and functionalization of gold nanoparticles in ionic liquids is also reported, wherein the colour of the gold nanoparticles can be tuned by changing the anion of ionic liquid.<sup>29</sup> Ru nanoparticles, stabilized by oligoethyleneoxythiol, are found to be soluble in both aqueous and organic media.<sup>30</sup> While Rh multipods are obtained through the seeded-growth mechanism on reducing  $\text{RhCl}_3$  in ethylene glycol in the presence of PVP,<sup>31</sup> Ir nanocrystals have been prepared by the reduction of an organometallic precursor in the presence of hexadecanediol and different capping agents.<sup>32</sup> Ru, Rh and Ir nanocrystals and other nanostructures are prepared by carrying out the decomposition of

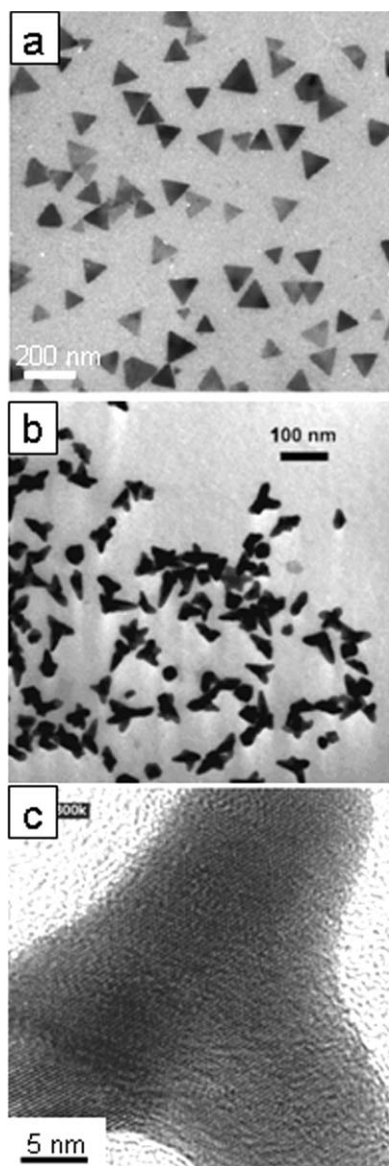


**Fig. 1** (a) Ag nanoprisms obtained by controlled irradiation of bis(*p*-sulfonatophenyl) phenylphosphine dihydrate dipotassium capped Ag nanocrystals. (b) Low and (c) high-magnification (scale bar = 5 nm) TEM images of branched Au nanocrystals. Fig. 1a reprinted with permission from Macmillan Publishers Ltd.: *Nature*, 2003, **425**, 487, © 2003. Fig. 1b reprinted with permission from E. Hao, R. C. Bailey and G. C. Schatz, *Nano Lett.*, 2004, **4**, 327. © 2004 American Chemical Society.

the respective metal acetylacetonates in a hydrocarbon (decalin or toluene) or an amine (*n*-octylamine or oleylamine) around 573 K.<sup>33</sup> Cobalt nanoparticles of ~3 nm diameter have been synthesized by the reaction of di-isobutyl aluminium hydride with Co-( $\eta^3$ -C<sub>8</sub>H<sub>15</sub>)( $\eta^4$ -C<sub>8</sub>H<sub>12</sub>) or Co[N(SiMe<sub>3</sub>)<sub>2</sub>]<sub>2</sub>.<sup>34</sup> Monodisperse Pt nanocrystals with cubic, cuboctahedral and octahedral shapes with diameters of ~9 nm have been obtained by the polyol process.<sup>35</sup> The polyol process has also been employed to obtain PtBi nanoparticles.<sup>36</sup> AuPt nanoparticles have been successfully incorporated in SiO<sub>2</sub> films.<sup>37</sup> FePt nanocubes with ~7 nm diameter (Fig. 3) have been synthesized by the reaction of the oleic acid and Fe(CO)<sub>5</sub> with benzyl ether/octadecene solution of Pt(acac)<sub>2</sub>.<sup>38</sup>

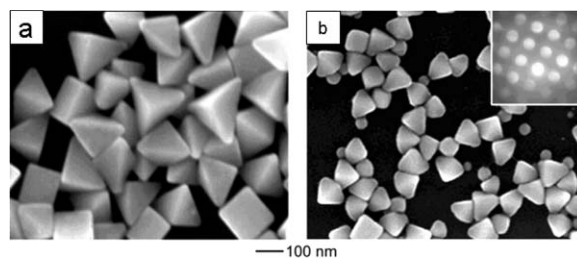


**Fig. 2** SEM images of right-bipyramids approximately (a) 150 nm and (b) 75 nm in edge length. The inset in (b) shows the electron diffraction pattern obtained from a single right-bipyramid, indicating that it is bounded by (100) facets. Reprinted with permission from B. J. Wiley, Y. Xiong, Z.-Y. Li, Y. Yin and Younan Xia, *Nano Lett.*, 2006, **6**, 765. © 2006 American Chemical Society.

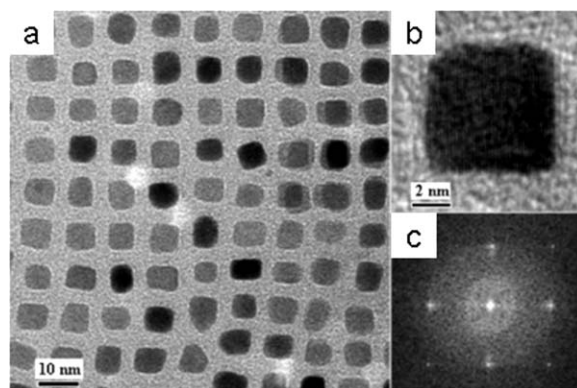


**Fig. 3** TEM bright field images of (a) 6.9 nm Fe<sub>30</sub>Pt<sub>50</sub> nanocubes; (b) HREM image of a single FePt nanocube; (c) Fast-Fourier transform (FFT) of the HREM in (b). Reprinted with permission from M. Chen, J. Kim, J. P. Liu, H. Fan and S. Sun, *J. Am. Chem. Soc.*, 2006, **128**, 7132. © 2006 American Chemical Society.

## 2.2 Metal oxides

Metal oxide nanocrystals are mainly prepared by the solvothermal decomposition of organometallic precursors. Solvothermal conditions afford high autogenous pressures inside the sealed autoclave that enable low-boiling solvents to be heated to temperatures well above their boiling points. Thus, reactions can be carried out at elevated temperatures and the products obtained are generally crystalline compared to those from other solution-based reactions.

Rockenberger *et al.*<sup>39</sup> described the use of cupferron complexes as precursors to prepare  $\gamma$ -Fe<sub>2</sub>O<sub>3</sub>, Cu<sub>2</sub>O and Mn<sub>3</sub>O<sub>4</sub> nanocrystals. CoO nanocrystals with diameters in 4.5–18 nm range have been prepared by the decomposition of cobalt cupferronate in decalin at 543 K under solvothermal conditions.<sup>40</sup> Magnetic measurements indicate the presence of ferromagnetic interaction in the small CoO nanocrystals. Nanocrystals of MnO and NiO are obtained from cupferronate precursors under solvothermal conditions.<sup>41</sup> The nanocrystals exhibit superparamagnetism accompanied by magnetic hysteresis below a blocking temperature. Nanocrystals of CdO and CuO are prepared by the solvothermal decomposition of metal-cupferronate in presence of trioctylphosphine oxide (TOPO) in toluene.<sup>42</sup> ZnO nanocrystals have been synthesized from the cupferron complex by a solvothermal route in toluene solution.<sup>43</sup>  $\gamma$ -Fe<sub>2</sub>O<sub>3</sub> and CoFe<sub>2</sub>O<sub>4</sub> nanocrystals can also be produced by the decomposition of the cupferron complexes.<sup>44</sup>

Metallic  $\text{ReO}_3$  nanocrystals with diameters in the 8.5–32.5 nm range are obtained by the solvothermal decomposition of the  $\text{Re}_2\text{O}_7$ -dioxane complex under solvothermal conditions.<sup>45</sup> Fig. 4a shows a TEM image of  $\text{ReO}_3$  nanocrystals of 17 nm average diameter with the size distribution histogram as an upper inset. The lower inset shows a HREM image of 8.5 nm nanocrystal. The nanocrystals exhibit a surface plasmon band around 520 nm which undergoes blue-shifts with decrease in size (Fig. 4b). Such blue-shifts in the  $\lambda_{\text{max}}$  with decreasing particle size is well-known in the case of metal nanocrystals.<sup>46</sup> Inset in Fig. 4b shows the photograph of four different sizes of  $\text{ReO}_3$  nanocrystals soluble in  $\text{CCl}_4$ . Surface-enhanced Raman scattering of pyridine, pyrazine and pyrimidine adsorbed on  $\text{ReO}_3$  nanocrystals has been observed.<sup>47</sup> Magnetic hysteresis is observed at low temperatures in the case of the 8.5 nm particles suggesting a superparamagnetic behaviour.

Apart from solvothermal methods, thermolysis of precursors in high boiling solvents, the sol-gel method, hydrolysis and use of micelles have been employed to synthesize the metal oxide nanocrystals. Thus, Park *et al.*<sup>48</sup> have used metal-oleates as precursors for the preparation of monodisperse  $\text{Fe}_3\text{O}_4$ ,  $\text{MnO}$  and  $\text{CoO}$  nanocrystals. 1-Octadecene, octyl ether and trioctylamine have been used as solvents. Hexagonal and cubic  $\text{CoO}$  nanocrystals can be prepared by the decomposition of cobalt acetylaceto-

nate in oleylamine under kinetic and thermodynamic conditions respectively.<sup>49</sup> Hexagonal pyramid-shaped  $\text{ZnO}$  nanocrystals have been obtained by the thermolysis of the  $\text{Zn}$ -oleate complex.<sup>50</sup>  $\text{ZnO}$  nanocrystals have been prepared from zinc acetate in 2-propanol by the reaction with water.<sup>51</sup>  $\text{ZnO}$  nanocrystals with cone (Fig. 5), hexagonal cone and rod shapes have been obtained by the non-hydrolytic ester elimination sol-gel reactions.<sup>52</sup> In this reaction,  $\text{ZnO}$  nanocrystals with various shapes were obtained by the reaction of zinc acetate with 1,12-dodecanediol in the presence of different surfactants. In this laboratory, it has been found that reactions of alcohols such as ethanol and *t*-butanol with  $\text{Zn}$  powder readily yield  $\text{ZnO}$  nanocrystals.<sup>53</sup>

Nanocrystals of  $\text{BaTiO}_3$  are obtained by the thermal decomposition of MOCVD reagents (alkoxides such as  $\text{BaTi}(\text{O}_2\text{CC}_7\text{H}_{15})[\text{OCH}(\text{CH}_3)_2]_5$ ) in diphenyl ether containing oleic acid, followed by the oxidation of the product with  $\text{H}_2\text{O}_2$ .<sup>54</sup> Thermal decomposition of uranyl acetylacetonate in a mixture solution of oleic acid, oleylamine, and octadecene at 423 K gives uranium oxide nanocrystals.<sup>55</sup> Treatment of metal acetylacetonates under solvothermal conditions produces nanocrystals of metal oxides such as  $\text{Ga}_2\text{O}_3$ ,  $\text{ZnO}$  and cubic  $\text{In}_2\text{O}_3$ .<sup>56</sup> Nearly monodisperse  $\text{In}_2\text{O}_3$  nanocrystals have been obtained starting with indium acetate, oleylamine and oleic acid.<sup>57</sup>  $\text{TiO}_2$  nanocrystals can be prepared

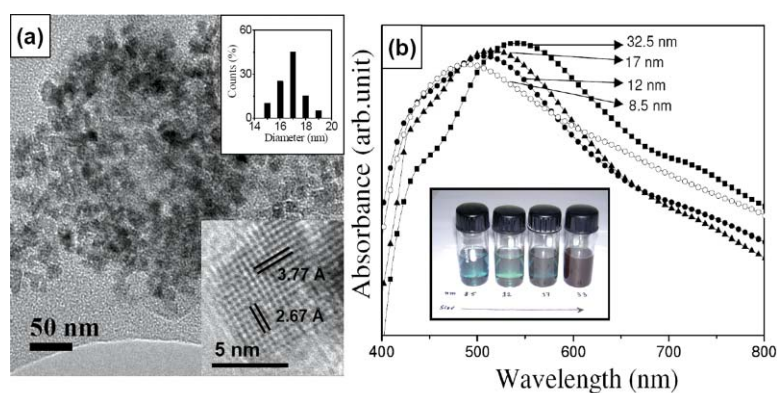


**Fig. 4** (a) TEM image of  $\text{ReO}_3$  nanocrystals of average diameter 17 nm. Upper inset shows the size distribution histogram. Lower inset shows the HREM image of a single 8.5 nm nanocrystal. (b) Optical absorption spectra of  $\text{ReO}_3$  nanocrystals with average diameters of 8.5, 12, 17 and 32.5 nm. Inset in (b) shows a picture of four different sizes of  $\text{ReO}_3$  nanocrystals dissolved in  $\text{CCl}_4$ . Reprinted with permission from K. Biswas and C. N. R. Rao, *J. Phys. Chem. B*, 2006, **110**, 842. © 2006 American Chemical Society.

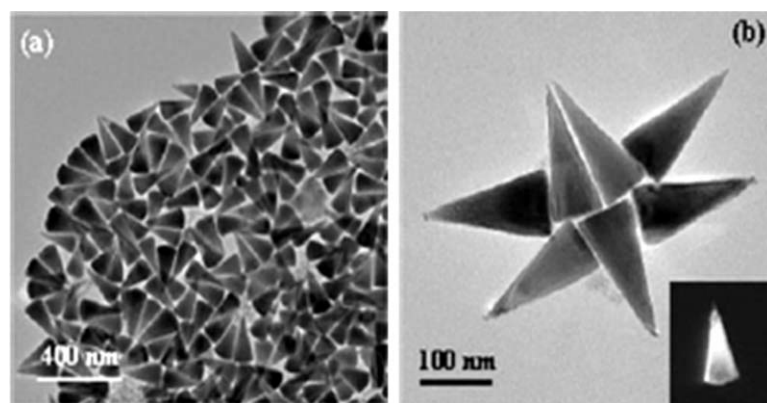


**Fig. 5** (a) and (b) TEM images of cone-shaped  $\text{ZnO}$  nanocrystal. Inset in (b) shows a dark field image of a single cone-shaped nanocrystal. Reproduced with permission from J. Joo, S. G. Kwon, J. H. Yu and T. Hyeon, *Adv. Mater.*, 2005, **17**, 1873. © 2005 Wiley-VCH Verlag GmbH & Co. KGaA.

by the low-temperature reaction of low-valent organometallic precursors.<sup>58</sup> Pure anatase TiO<sub>2</sub> nanocrystals have been prepared by the hydrolysis of TiCl<sub>4</sub> with ethanol at 273 K followed by calcination at 360 K for 3 days.<sup>59</sup> The growth kinetics and the surface hydration chemistry have also been investigated. Pileni and co-workers<sup>60,61</sup> have pioneered the use of oil in water micelles to prepare particles of CoFe<sub>2</sub>O<sub>4</sub>,  $\gamma$ -Fe<sub>2</sub>O<sub>3</sub>, and Fe<sub>3</sub>O<sub>4</sub>. The basic reaction involving hydrolysis is now templated by a micellar droplet. The reactants are introduced in the form of a salt of a surfactant such as sodium dodecylsulfate (SDS). Thus, by adding CH<sub>3</sub>NH<sub>3</sub>OH to a micelle made of calculated quantities of Fe(SDS)<sub>2</sub> and Co(SDS)<sub>2</sub>, nanocrystals of CoFe<sub>2</sub>O<sub>4</sub> are obtained.

### 2.3 Metal chalcogenides

Nearly monodisperse Cd-chalcogenide nanocrystals (CdE; E = S, Se, Te) have been synthesized by the injection of organometallic reagents such as alkylcadmium into a hot coordinating solvent in the presence of silylchalcogenides/phosphinechalcogenides.<sup>62</sup> Alivisatos and coworkers<sup>63</sup> have produced Cd-chalcogenide nanocrystals by employing tri-butylphosphine at higher temperatures. Nanocrystals of metal chalcogenides are generally prepared by the reaction of metal salts with an appropriate sulfiding or seleniding agent under solvothermal or thermolysis conditions. Thus, toluene-soluble CdSe nanocrystals with a diameter of 3 nm have been prepared solvothermally by reacting cadmium stearate with elemental Se in toluene in the presence of tetralin.<sup>64</sup> The key step in the reaction scheme is the aromatization of tetralin to naphthalene in the presence of Se, producing H<sub>2</sub>Se. Organic-soluble CdS nanocrystals are similarly prepared by the reaction of a cadmium salt with S in toluene in the presence of tetralin.<sup>65</sup> Fig. 6 shows the TEM images and electron diffraction patterns of TOPO-capped CdS nanocrystals prepared by this method. PbS and PbSe crystallites and nanorods can also be prepared by this method.<sup>66</sup> Nanocrystals of the transition metal dichalcogenides

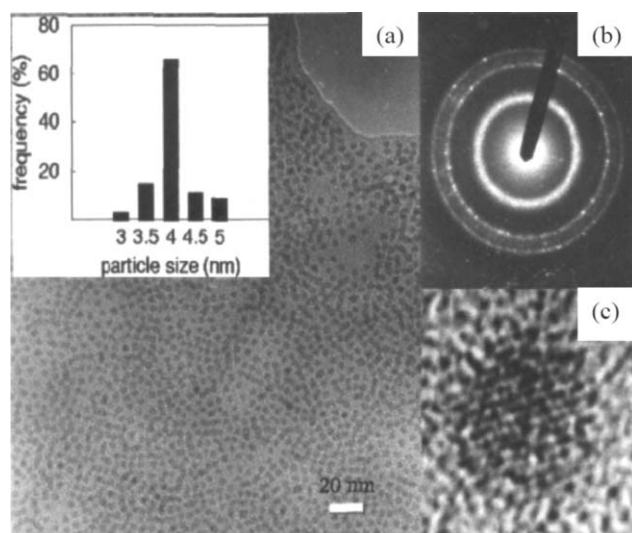


**Fig. 6** (a) TEM image of TOPO-capped CdS particles. Inset shows the size distribution of the nanocrystals. The electron diffraction pattern of the nanocrystals is shown in (b) and a HREM image of a nanocrystal is shown in (c). Reprinted from U. K. Gautam, R. Seshadri and C. N. R. Rao, *Chem. Phys. Lett.*, 2003, **375**, 560, © 2003 with permission from Elsevier. <http://www.sciencedirect.com/science/journal/00092614>

(ME<sub>2</sub>; M = Fe, Co, Ni, Mo; E = S or Se) with diameters in the range 4–200 nm have been prepared by a hydrothermal route.<sup>67</sup>

Peng *et al.*<sup>68–71</sup> have proposed the use of greener Cd sources such as cadmium oxide, carbonate and acetate instead of the dimethylcadmium. These workers suggest that the size distribution of the nanocrystals is improved by the use of hexadecylamine, a long-chain phosphonic acid or a carboxylic acid. The method can be extended to prepare CdS nanoparticles by the use of tri-*n*-octylphosphine sulfide (TOP-S) and hexyl or tetradecyl phosphonic acid in mixture with TOPO–TOP. Hyeon and co-workers<sup>72</sup> have prepared nanocrystals of several metal sulfides such as CdS, ZnS, PbS, and MnS with different shapes and sizes by the thermolysis of metal–oleylamine complexes in the presence of S and oleylamine (Fig. 7).

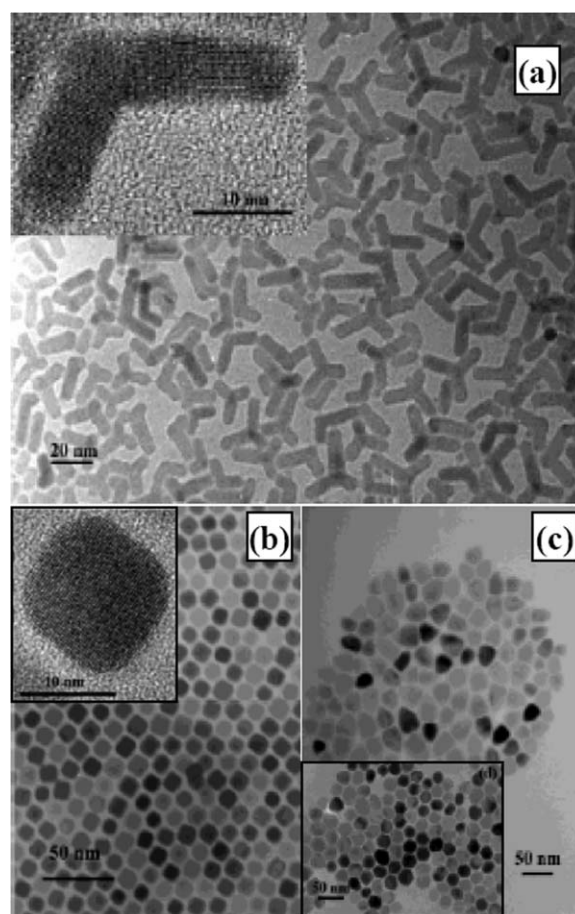


**Fig. 7** (a) TEM images of a mixture of rods, bipods, and tripods of CdS nanocrystals with an average size of 5.4 nm (thickness) 20 nm (length). Inset is a HREM image of a single CdS bipod-shaped nanocrystal. (b) Low-magnification TEM image of 13 nm PbS nanocrystals. Inset shows a HREM image of a single 13 nm PbS nanocrystal. (c) Short bullet-shaped MnS nanocrystals. Inset shows hexagon-shaped MnS nanocrystals. Reprinted with permission from J. Joo, H. B. Na, T. Yu, J. H. Yu, Y. W. Kim, F. Wu, J. Z. Zhang and T. Hyeon, *J. Am. Chem. Soc.*, 2003, **125**, 11100. © 2003 American Chemical Society.

CdSe and CdTe nanocrystals can be prepared without precursor injection.<sup>73</sup> The method involves refluxing the cadmium precursor with Se or Te in octadecene. CdSe nanocrystals have also been synthesized using elemental selenium dispersed in octadecene

without the use of trioctylphosphine.<sup>74</sup> ZnSe nanocrystals have been prepared in a hot mixture of a long-chain alkylamine and alkylphosphines.<sup>75</sup> Highly monodisperse cubic-shaped PbTe nanocrystals (Fig. 8) have been prepared with size distributions less than 7% by a rapid injection technique.<sup>76</sup> PbS nanocrystals are obtained by reacting the PbCl<sub>2</sub>-oleylamine complex with the S-oleylamine complex without the use of any solvent.<sup>77</sup> Homogeneously alloyed CdS<sub>x</sub>Se<sub>1-x</sub> ( $x = 0-1$ ) nanocrystals are prepared by the thermolysis of metal-oleylamine complexes in the presence of S and Se.<sup>78</sup> The band gap of these nanocrystals can be tuned by varying the composition. Thermolysis of a mixture composed of Cu and In oleates in alkanethiol yields copper indium sulfide nanocrystals with acorn, bottle, and larva shapes.<sup>79</sup> Nanocrystals of Ni<sub>3</sub>S<sub>4</sub> and Cu<sub>1-x</sub>S have been prepared by adding elemental sulfur to metal precursors dissolved in dichlorobenzene or oleylamine at relatively high temperatures.<sup>80</sup>

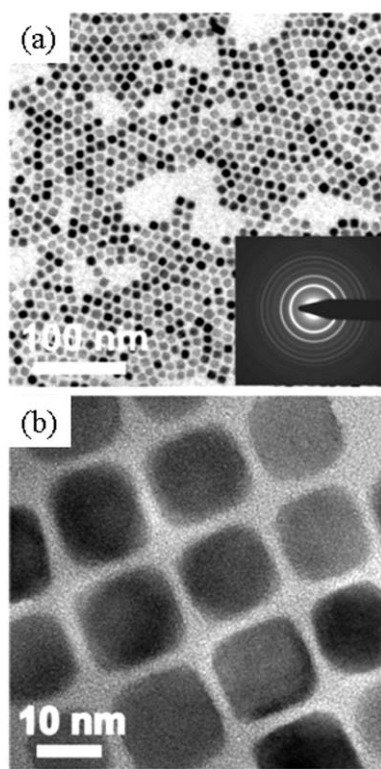


**Fig. 8** (a) TEM image of as-prepared cube-like PbTe nanocrystals. Inset shows the SAED pattern. (d) Ordered array consisting of 15 nm cubic-shaped PbSe nanocrystals after size selective precipitation. Reprinted with permission from J. E. Murphy, M. C. Beard, A. G. Norman, S. P. Ahrenkiel, J. C. Johnson, P. Yu, O. I. Mićić, R. J. Ellingson and A. J. Nozik, *J. Am. Chem. Soc.*, 2006, **128**, 3241. © 2006 American Chemical Society.

Decomposition of single molecular precursors provides convenient and effective routes for the synthesis of metal chalcogenide nanocrystals. In this method, a molecular complex consisting of both the metal and the chalcogen is thermally decomposed in a coordinating solvent. For example dithiocarbamates and diselenocarbamates have been found to be good air stable precursors for sulfides and selenides of Cd, Zn and Pb.<sup>81</sup> Nanocrystals of Cd, Hg, Mn, Pb, Cu, and Zn sulfides have been obtained by thermal decomposition of metal hexadecylxanthates in hexadecylamine

and other solvents at relatively low temperatures (323–423 K) under ambient conditions.<sup>82</sup>

Hexagonal CdS nanocrystals have been obtained by the reaction of cadmium acetate dihydrate with thioacetamide in imidazolium[BMIM]-based ionic liquids.<sup>83</sup> Fig. 9(a) shows the TEM image along with HREM image as a top inset of CdS nanocrystals prepared in [BMIM][MeSO<sub>4</sub>]. Particle size of the CdS nanoparticles varies between 3 and 13 nm with the anion of imidazolium based ionic liquid under the same reaction conditions. Addition of TOPO to the reaction mixture causes greater monodispersity as well as smaller particle size. Hexagonal ZnS and cubic PbS nanoparticles with average diameters of 3 and 10 nm respectively have been prepared by the reaction of the metal acetates with thioacetamide in [BMIM][BF<sub>4</sub>]. Hexagonal CdSe nanocrystals with an average diameter of 12 nm were obtained by the reaction of cadmium acetate dihydrate with dimethylselenourea in [BMIM][BF<sub>4</sub>]. CdSe nanocrystals have also been prepared using the phosphonium ionic liquid trihexyl(tetradecyl)phosphoniumbis(2,4,4 trimethylpentylphosphinate) as a solvent and capping agent.<sup>84</sup>

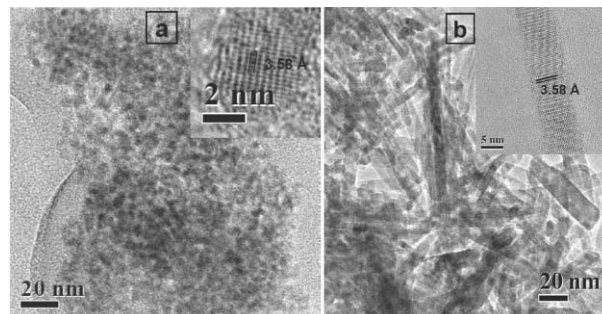
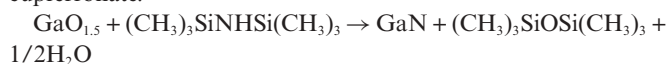


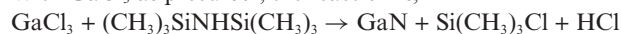
**Fig. 9** (a) TEM images of 4 nm CdS nanoparticles prepared in [BMIM][MeSO<sub>4</sub>]. Insets show a HREM image of the 4 nm CdS nanoparticle. (b) TEM image of CdS nanorods prepared in a [BMIM][BF<sub>4</sub>] and ethylenediamine mixture. Inset shows a HREM image of a nanorod. Reproduced with permission from K. Biswas and C. N. R. Rao, *Chem.–Eur. J.*, 2007, **13**, 6123. © 2007 Wiley-VCH Verlag GmbH & Co. KGaA.

## 2.4 Metal pnictides

Large GaN nanocrystals (32 nm) were prepared by Xie *et al.*,<sup>85</sup> by treating GaCl<sub>3</sub> with Li<sub>3</sub>N in benzene under solvothermal conditions. GaN nanocrystals of various sizes have been prepared under solvothermal conditions, by employing gallium cupferronate or chloride as the gallium source and 1,1,1,3,3,3-hexamethyldisilazane (HMDS) as the nitrating agent and toluene as solvent.<sup>86</sup> By employing surfactants such as cetyltrimethylammonium bromide (CTAB), the size of the nanocrystals could be controlled (Fig. 10a). In the case of cupferronate, the formation of the nanocrystals is likely to involve nitridation of the nascent gallium oxide nanoparticles formed by the decomposition of the cupferronate.



With GaCl<sub>3</sub> as precursor, the reaction is,



This method has been applied for the synthesis of AlN and InN nanocrystals (Fig. 10b).<sup>87</sup> The procedure yields nanocrystals with an average diameter of 10 nm for AlN, 15 nm for InN and as low

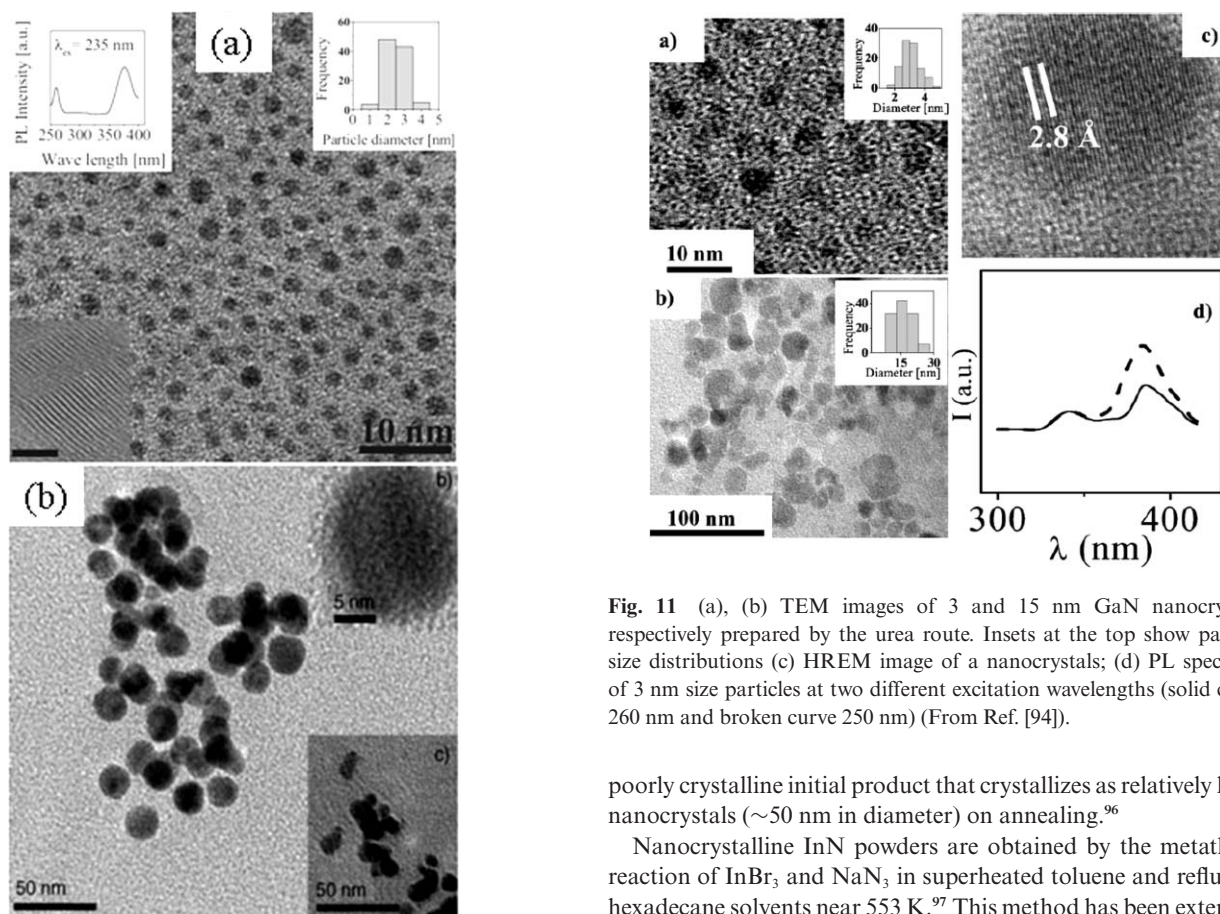


**Fig. 10** (a) TEM image of CTAB-capped 2.5 nm GaN nanocrystals prepared starting with Ga cupferron. The upper right inset shows the size distribution. The lower inset shows a HREM image (scale bar is 2 nm) and upper inset also shows the PL spectrum of CTAB capped 2.5 nm GaN nanocrystals; (b) TEM image of InN nanocrystals of 15 nm average diameter prepared starting with In cupferron. The upper inset shows a HREM image of a single nanocrystal. The lower inset shows a TEM image of InN nanocrystals prepared starting with InCl<sub>3</sub>. Reproduced with permission from K. Sardar and C. N. R. Rao, *Adv. Mater.*, 2004, **16**, 425 and K. Sardar, F. L. Deepak, A. Govindaraj, M. M. Seikh and C. N. R. Rao, *Small*, 2005, **1**, 91. © 2004 and 2005 Wiley-VCH Verlag GmbH & Co. KGaA.

as 4 nm for GaN. Indium-doped GaN nanocrystals with 5% and 10% In as well as 3% and 5% Mn-doped GaN nanocrystals have been prepared by this method.<sup>88,89</sup>

GaN nanocrystals have also been obtained by the thermal decomposition of precursor compounds such as (C<sub>2</sub>H<sub>5</sub>)<sub>3</sub>N·Ga(N<sub>3</sub>)<sub>3</sub> and polymeric [Ga(NH)<sub>3/2</sub>]<sub>n</sub>.<sup>90–92</sup> Thus, by the thermolysis of azido compounds, Manz *et al.*<sup>93</sup> have obtained nanocrystals of hexagonal GaN of varying diameters. Group 13 metal nitrides (GaN, AlN, InN) have been prepared by a single source precursor route.<sup>94</sup> The precursors are the adducts of the metal chlorides and urea. Hexagonal nanocrystals of GaN, AlN, and InN were obtained by refluxing the precursors in tri-*n*-octylamine. Fig. 11 shows the TEM images and the PL spectrum of GaN nanocrystals prepared by the urea route. This method has also been extended for the synthesis of BN, TiN and NbN nanoparticles.<sup>95</sup> Solvothermal synthesis involving the reaction of GaCl<sub>3</sub> and NaN<sub>3</sub> yields a

**Fig. 11** (a), (b) TEM images of 3 and 15 nm GaN nanocrystals respectively prepared by the urea route. Insets at the top show particle size distributions (c) HREM image of a nanocrystals; (d) PL spectrum of 3 nm size particles at two different excitation wavelengths (solid curve 260 nm and broken curve 250 nm) (From Ref. [94]).

poorly crystalline initial product that crystallizes as relatively large nanocrystals (~50 nm in diameter) on annealing.<sup>96</sup>

Nanocrystalline InN powders are obtained by the metathesis reaction of InBr<sub>3</sub> and NaN<sub>3</sub> in superheated toluene and refluxing hexadecane solvents near 553 K.<sup>97</sup> This method has been extended to prepare Ga<sub>1-x</sub>In<sub>x</sub>N ( $x = 0.5$  and  $0.75$ ) nanocrystals. A benzene-thermal route has been developed to prepare nanocrystalline InN at 453–473K by choosing NaNH<sub>2</sub> and In<sub>2</sub>S<sub>3</sub> as novel nitrogen and indium sources.<sup>98</sup> This route has been extended to synthesize other group III nitrides. AlN nanocrystals have been prepared by the benzene-thermal reaction between AlCl<sub>3</sub> and Li<sub>3</sub>N.<sup>99</sup>

An early procedure for the preparation of phosphides and arsenides of gallium, indium and aluminium involved the dehydro-silylation reaction. Alivisatos and co-workers<sup>100</sup> adapted this method to prepare GaAs nanoparticles using GaCl<sub>3</sub> and As(SiMe<sub>3</sub>)<sub>3</sub> in quinoline. Using a similar scheme, GeSb, InSb, InAs, and InP nanocrystals were obtained.<sup>101</sup> This method has been modified to prepare InP, InAs, GaP, and GaInP<sub>2</sub> nanocrystals as well.<sup>102–104</sup> In a typical reaction, InCl<sub>3</sub> is complexed with TOPO/TOP and is reacted with a silylated pnictide such as E(SiMe<sub>3</sub>)<sub>3</sub> (E = As, P) at 536 K, followed by growth at elevated temperatures for several days. Phase-pure FeP nanocrystals have been synthesized by the reaction of iron(III) acetylacetonate with tris(trimethylsilyl)phosphine at temperatures of 513–593 K using trioctylphosphine oxide as a solvent and dodecylamine, myristic acid, or hexylphosphonic acid as additional capping groups (ligands).<sup>105</sup> The treatment of Mn<sub>2</sub>(CO)<sub>10</sub> with P(SiMe<sub>3</sub>)<sub>3</sub> in (TOPO)/myristic acid at elevated temperatures produced MnP as discrete nanocrystals.<sup>106</sup> In the presence of a surfactant, potassium stearate, quantum-confined InP nanocrystals were hydrothermally synthesized in aqueous ammonia.<sup>107</sup> High quality InP nanocrystals are obtained by the reaction of (Me)<sub>3</sub>In and P(SiMe<sub>3</sub>)<sub>3</sub> in a coordinating ester solvent.<sup>108</sup> O'Brien and co-workers developed a single molecular precursor route to synthesize InP and GaP

nanocrystals using diorganophosphides- $M(\text{PBUt}_2)_3$  ( $M=\text{Ga}, \text{In}$ ). This method has also been adapted to synthesize  $\text{Cd}_3\text{P}_2$  using  $[\text{MeCdP}(\text{BUt})_2]_3$ . The dimer  $[\text{t-Bu}_2\text{AsInEt}_2]_2$  has been synthesized and used as a single-source organometallic precursor to grow InAs nanocrystals.<sup>109</sup> Reduction of transition metal pnictates yields metal pnictides. Using this method nanoparticle of FeP,  $\text{Fe}_2\text{P}^{110}$  and NiAs<sup>111</sup> has been prepared. Monodisperse iron, cobalt and nickel monoarsenide nanocrystals were obtained under high-intensity ultrasonic irradiation from the reaction of transition metal chlorides, arsenic and zinc in ethanol.<sup>112</sup>

### 3. Core@shell nanoparticles

Core@shell particles involving metal, semiconductor or oxide nanocrystals in the core, with shells composed of different materials have been investigated widely.<sup>113</sup> The method of Murray *et al.*<sup>62</sup> involving the decomposition of dimethyl cadmium has been adapted to synthesize nanocrystals of the type  $\text{CdSe@ZnS}$ ,  $\text{CdSe@ZnSe}$ , and  $\text{CdSe@CdS}$ .<sup>114</sup> Core@shell growth is achieved by injecting the precursors forming the shell materials into a dispersion containing the core nanocrystals. The injection is carried out at a slightly lower temperature to force shell growth, avoiding independent nucleation. Thus, a mixture of diethylzinc and bis(trimethylsilyl)sulfide is injected into a hot solution containing the core CdSe nanocrystals to encase them with a ZnS layer.<sup>115</sup> O'Brien and co-workers<sup>116</sup> have used single-source methods to prepare core@shell nanocrystals. By successive thermolysis of unsymmetrical diseleno and dithiocarbamates, core@shell nanocrystals of the type  $\text{CdSe@ZnS}$  and  $\text{CdSe@ZnSe}$  have been prepared.<sup>116</sup>  $\text{CdSe@CdS}$  core@shell nanoparticles with a core diameter of  $\sim 1.5$  nm have been prepared at the liquid-liquid interface starting with cadmium myristate and oleic acid in toluene and selenourea/thiourea in the aqueous medium.<sup>117</sup> Luminescent multi-shell nanocrystals of the composition  $\text{CdSe-core CdS/Zn}_{0.5}\text{Cd}_{0.5}\text{S/ZnS-shell}$  have been prepared by successive ion layer adhesion and reaction technique,<sup>118</sup> where in the growth of the shell is carried out one monolayer at a time, by alternately injecting cationic and anionic precursors into the reaction mixture with core nanocrystals. Water-soluble  $\text{CdSe@CdS}$  core@shell nanocrystals with dendron carbohydrate anchoring groups have been prepared.<sup>119</sup> Cao and Banin<sup>120</sup> have successfully coated InAs nanocrystals with shells of InP, GaAs, CdSe, ZnSe, and ZnS. In Fig. 12, we show the TEM and HREM images of  $\text{InAs@InP}$  and  $\text{InAs@CdSe}$  core@shell nanocrystals. Using the shell layers, the bandgap of InAs can be tuned in the near-IR region.

Metal on metal core@shell structures provide a means for generating metal nanocrystals with varied optical properties. Morriss and Collins<sup>121</sup> prepared  $\text{Au@Ag}$  nanocrystals by reducing Au with P by the Faraday's method and Ag with hydroxylamine hydrochloride. They observed a progressive blue shift of the Au plasmon band with incorporation of Ag, accompanied by a slight broadening. For sufficiently thick shells, the plasmon band resembled that of pure Ag particles. Large Au nanoparticles prepared by the citrate method have been used as seeds for the reduction of Ag nanocrystals using ascorbic acid, with CTAB as the capping agent.<sup>122</sup>  $\text{Au@Ag}$  as well as  $\text{Ag@Au}$  nanocrystals were prepared by the sequential reduction using sodium citrate.<sup>123</sup>  $\text{Au@Ag}$  as well as  $\text{Ag@Au}$  nanoparticles are also prepared by a UV-photoactivation technique.<sup>124</sup> Mirkin and co-workers<sup>125</sup> have

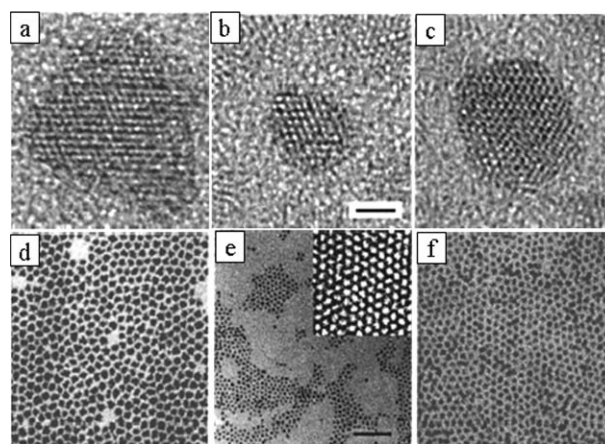


**Fig. 12** HREM images of  $\text{InAs@InP}$  core@shell (frame (a), core radius 1.7 nm, shell thickness 2.5 nm), InAs core ((b), core radius 1.7 nm), and  $\text{InAs@CdSe}$  core@shell ((c), core radius 1.7 nm, shell thickness 1.5 nm). The scale bar is 2 nm. (d), (e) and (f) are low magnification TEM images of  $\text{InAs@InP}$ , InAs core and  $\text{InAs@CdSe}$  core/shell nanoparticles respectively. The scale bar is 50 nm. The inset in (e) ( $70 \times 70$  nm), displays a portion of a superlattice structure formed from the InAs cores. Reprinted with permission from Y.-W. Cao and U. Banin, *J. Am. Chem. Soc.*, 2000, **122**, 9692. © 2000 American Chemical Society.

coated Ag nanocrystals with a thin Au shell to provide stability against precipitation under physiological conditions. A thin shell has little effect on the optical properties.  $\text{Au@Pd}$  nanoparticles with controllable size from 35 to 100 nm were prepared by the chemical deposition of Pd over pre-formed 12 nm Au seeds.<sup>126</sup> Reactive magnetic nanocrystals are rendered passive and made easy to handle by coating them with a layer of noble metals. For example, a layer of Ag was grown *in situ* on Fe and Co nanocrystals synthesized using reverse micelles.<sup>127</sup> A similar procedure has been used to coat Au as well.<sup>128</sup>  $\text{Fe@Au}$  nanocrystals are also prepared by sequential citrate reduction followed by magnetic separation.<sup>129</sup>  $\text{Fe@Au}$  nanocrystals were synthesized by a wet chemical procedure involving laser irradiation of Fe nanoparticles and Au powder in a liquid medium.<sup>130</sup> The nanoparticles were superparamagnetic with a blocking temperature of 170 K.  $\text{Fe}_3\text{O}_4$  of selected size were used as seeding materials for the reduction of Au precursors to produce monodisperse  $\text{Fe}_3\text{O}_4@Au$  nanoparticles.<sup>131</sup>

A dielectric oxide layer (*e.g.* silica) is useful as a shell material because of the stability it lends to the core and its optical transparency. The classic method of Stober for solution deposition of silica are adaptable for coating of nanocrystals with silica shells.<sup>132</sup> This method relies on the pH and the concentration of the solution to control the rate of deposition. The natural affinity of silica to oxidic layers has been exploited to obtain silica coating on a family of iron oxide nanoparticles including hematite and magnetite.<sup>133</sup> Such a deposition process is not readily extendable to grow shell layers on metals. The most successful method for silica encapsulation of metal nanoparticles is that due to Mulvaney and co-workers.<sup>134</sup> In this method, the surface of the nanoparticles is functionalized with aminopropyltrimethylsilane, a bifunctional molecule with a pendant silane group which is available for condensation of silica. The next step involves the slow deposition of silica in water followed by the fast deposition of silica in ethanol. Fig. 13 shows the TEM images



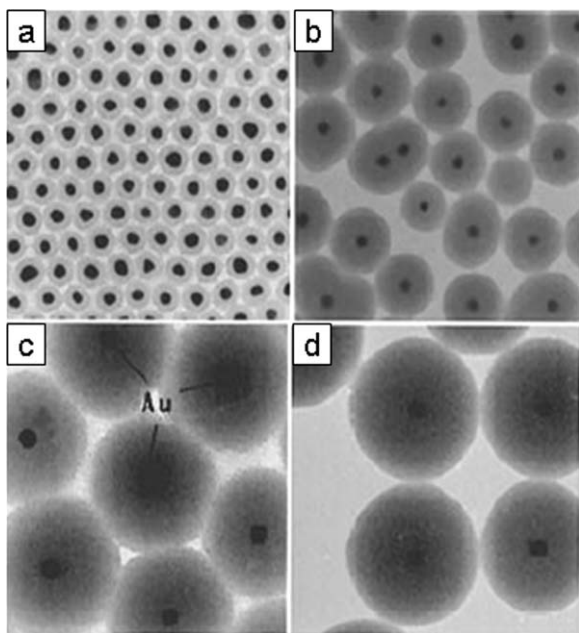


**Fig. 13** TEM images of Au@SiO<sub>2</sub> particles produced during the growth of the silica shell around 15 nm Au particles. The shell thicknesses are (a) 10 nm, (b) 23 nm, (c) 58 nm, and (d) 83 nm. Reprinted with permission from L. M. Liz-Marzán, M. Giersig and P. Mulvaney, *Langmuir*, 1996, **12**, 4329. © 1996 American Chemical Society.

of Au@SiO<sub>2</sub> nanocrystals with various shell thickness reported by Mulvaney's group.<sup>135</sup> Au@TiO<sub>2</sub> core@shell nanocrystals have been prepared by complexation of a negatively charged titanium precursor, titanium(IV) bis(ammonium lactato)dihydroxide, with poly(dimethyldiallylammonium chloride).<sup>136</sup> Silver nanoparticles coated with a uniform, thin shell of titanium dioxide have been synthesized by a one-pot route, where the reduction of Ag<sup>+</sup> to Ag<sup>0</sup> and the controlled polymerization of TiO<sub>2</sub> on the surface of silver crystallites occurs simultaneously.<sup>137</sup> Pradeep and co-workers<sup>138,139</sup> have coated Au and Ag nanoparticles with TiO<sub>2</sub> and ZrO<sub>2</sub> in a single-step process.

ReO<sub>3</sub>@Au (Fig. 14a) and ReO<sub>3</sub>@Ag were prepared by the reduction of metal salts over ReO<sub>3</sub> nanoparticle seeds.<sup>140</sup> ReO<sub>3</sub>@SiO<sub>2</sub> and ReO<sub>3</sub>@TiO<sub>2</sub> (Fig. 14b) core-shell nanocrystals were prepared by hydrolysis of the organometallic precursors over the ReO<sub>3</sub> nanoparticles. ReO<sub>3</sub>@Au and ReO<sub>3</sub>@Ag core-shell nanoparticles show composite plasmon absorption bands comprising contributions from both ReO<sub>3</sub> and Au (Ag) (Fig. 14c) whereas ReO<sub>3</sub>@SiO<sub>2</sub> and ReO<sub>3</sub>@TiO<sub>2</sub> show shifts in the plasmon bands depending on the refractive index of the shell material (Fig. 14d). Co@SiO<sub>2</sub> nanocrystals were prepared combining the sodium borohydride reduction in aqueous solution, the Stober method, and/or the layer-by-layer self-assembly technique.<sup>141</sup> Nanocrystals with the ferrimagnetic CoFe<sub>2</sub>O<sub>4</sub> core and the antiferromagnetic MnO shell have been obtained by a high-temperature decomposition route with seed-mediated growth.<sup>142</sup>

## 4. Nanowires

There has been considerable interest in the synthesis, characterization and properties of nanowires of various inorganic materials.<sup>4,143,144</sup> Nanowires have been prepared using vapour phase

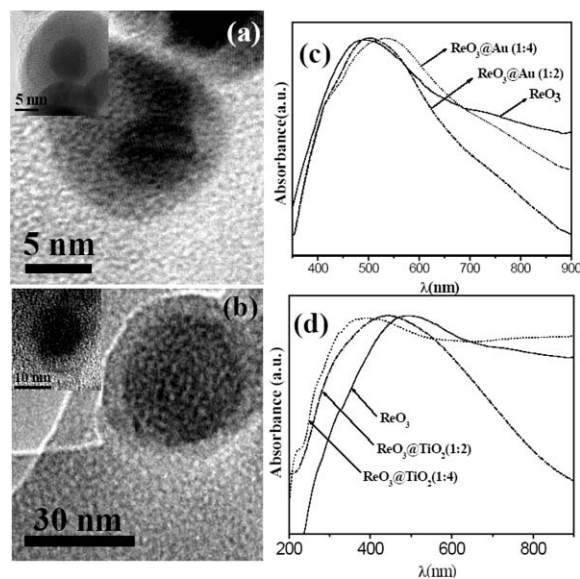


**Fig. 14** TEM images of core-shell nanoparticles of (a) ReO<sub>3</sub>@Au formed with a 5 nm ReO<sub>3</sub> particle. Inset shows ReO<sub>3</sub>@Au formed over an 8 nm ReO<sub>3</sub> particle. (b) ReO<sub>3</sub>@TiO<sub>2</sub> core-shell nanoparticle formed over a 32 nm ReO<sub>3</sub> particle with the inset showing a core-shell nanoparticle formed over a 12 nm ReO<sub>3</sub> nanoparticle. UV-visible absorption spectra of (c) ReO<sub>3</sub>@Au core-shell nanoparticles (1 : 2 and 1 : 4), and (d) ReO<sub>3</sub>@TiO<sub>2</sub> core-shell nanoparticles (1 : 2 and 1 : 4) with a 12 nm ReO<sub>3</sub> particle (From Ref. [140]).

methods such as vapour-liquid-solid (VLS) growth, vapour-solid (VS) growth, oxide-assisted growth and the use of carbothermal reactions. A variety of solution methods such as seed-assisted growth, polyol method, and oriented attachment have also been developed for the synthesis of one-dimensional nanostructures.

### 4.1 Metals

Metal nanowires are commonly prepared using templates such as anodic alumina or polycarbonate membranes, carbon nanotubes and mesoporous carbon.<sup>145-148</sup> The nanoscale channels are first impregnated with metal salts and the nanowires obtained by reduction, followed by the dissolution of the template. Nanowires of metals and semiconductors have also been grown electrochemically. This method has been employed to prepare linear Au-Ag nanoparticle chains.<sup>149</sup> Here, sacrificial Ni segments are placed between segments of noble metals (Au, Ag). The template pore diameter fixes the nanowire width, and the length of each metal segment is independently controlled by the amount of current passed before switching to the next plating solution for deposition of the subsequent segments. Nanowires are released by the dissolution of the template, and subsequently coated with the SiO<sub>2</sub>.

Au nanorods and nanowires have been alternatively prepared by a simple solution based reduction method making use of nanoparticle seeds.<sup>150</sup> Au nanoparticles with ~4 nm diameter react with the metal salt along with the weak reducing agent such as ascorbic acid in the presence of a directing surfactant yielding Au nanorods. This method was extended to prepare dog-bone like nanostructures.<sup>151</sup> The reaction is carried out in two-steps, wherein the first step involves the addition of an insufficient amount of ascorbic acid to the growth solution, leaving some unreacted metal salt after the reaction, which is later deposited on the Au nanorods

by the second addition of ascorbic acid. Addition of nitric acid enhances the proportion of Au nanorods with high aspect ratios ( $\sim 20$ ) in seed-mediated synthesis.<sup>152</sup> The growth of Au nanorods by the seed-assisted method does not appear to follow any reaction-limited or diffusion limited growth mechanism.<sup>153</sup>

A layer-by-layer deposition approach has been employed to produce polyelectrolyte-coated gold nanorods.<sup>154</sup> Au-nanoparticle-modified enzymes act as biocatalytic inks for growing Au or Ag nanowires on Si surfaces by using a patterning technique such as dip-pen-nanolithography.<sup>155</sup> Single-crystalline Au nanorods shortened selectively by mild oxidation using 1 M HCl at 343 K.<sup>156</sup> Aligned Au nanorods can be grown on a silicon substrate by employing a simple chemical amidation reaction on  $\text{NH}_2$ -functionalized Si substrates.<sup>157</sup> A seed-mediated surfactant method using a cationic surfactant has been developed to obtain pentagonal silver nanorods.<sup>158</sup>

A popular method for the synthesis of metal nanowires is the use of the polyol process,<sup>159,160</sup> wherein the metal salt is reduced in the presence of PVP to yield nanowires of the desired metal. For example, Ag nanowires have been rapidly synthesized using a microwave-assisted polyol method.<sup>161</sup> CoNi nanowires are obtained by heterogeneous nucleation in liquid polyol.<sup>162</sup> While Bi nanowires have been prepared employing  $\text{NaBiO}_3$  as the bismuth source.<sup>163</sup> Pd nanobars are synthesized by varying the type and concentration of reducing agent as well as reaction temperature.<sup>164</sup>

Metal nanowires are obtained in good yields by the nebulized spray pyrolysis of a methanolic solution of metal acetates.<sup>165</sup> This method has been employed for the synthesis of single-crystalline nanowires of zinc, cadmium and lead (see Fig. 15). The nanowires seem to grow by the vapour–solid mechanism. ZnO nanotubes

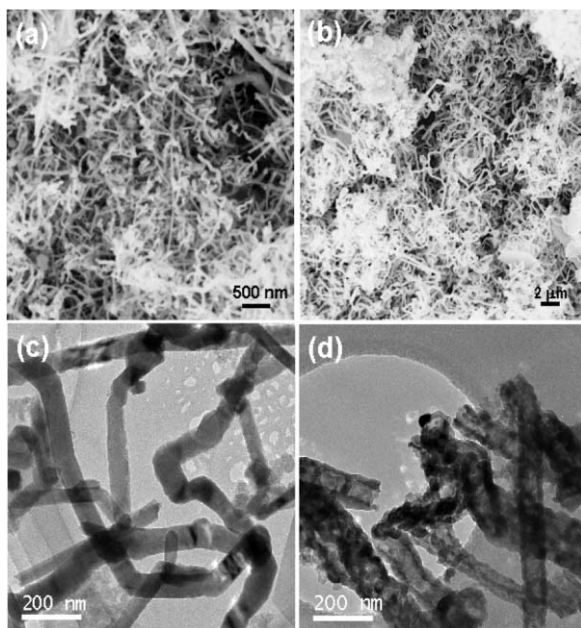


**Fig. 15** (a) and (b) SEM images of zinc and cadmium nanowires obtained by the pyrolysis of the corresponding metal acetates at 1173 K. (c) TEM image of zinc nanowires and (d) TEM image of ZnO nanotubes obtained by the oxidation of Zn nanowires at 723 K. Reproduced with permission from S. R. C. Vivekchand, G. Gundiah, A. Govindaraj and C. N. R. Rao, *Adv. Mater.*, 2004, **16**, 1842. © 2004 Wiley-VCH Verlag GmbH & Co. KGaA

shown in Fig. 15d can be obtained by the oxidation of zinc nanowires in air at 723 K.

## 4.2 Elemental semiconductors

Silicon nanowires with diameters in the 5–20 nm range have been prepared along with nanoparticles of 4 nm diameter by arc-discharge in water.<sup>166</sup> The Si nanowires shown in Fig. 16 were prepared in solution by using Au nanocrystals as seeds and silanes as precursors by the VLS mechanism.<sup>167</sup> Aligned Si nanowires are obtained by chemical vapour deposition (CVD) of  $\text{SiCl}_4$  on a gold colloid deposited Si(111) substrate.<sup>168</sup> Gold colloids have been used for nanowire synthesis by the VLS growth mechanism. Using anodic alumina membranes as templates, Si nanowires have been synthesized on Si substrates.<sup>169</sup> In this method, porous anodic alumina is grown on the Si substrate followed by the electrodeposition of the gold catalyst. Epitaxial Si nanowires are then obtained subsequently by VLS growth. Presence of oxygen is important for the growth of long untapered Si nanowires by the VLS mechanism.<sup>170</sup>

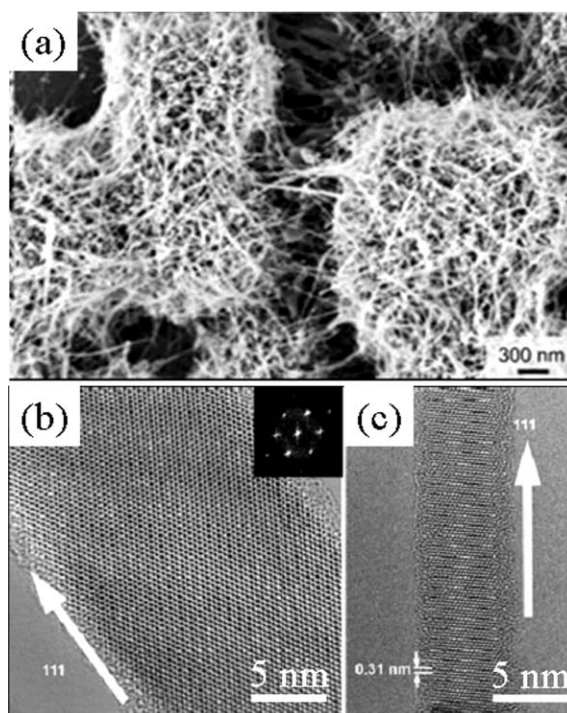


**Fig. 16** (a) SEM image of Si nanowires produced from Au nanocrystals and diphenylsilane at 723 K. (b), (c) HREM images of Si showing predominantly  $\langle 111 \rangle$  orientation. Inset in (b) shows a FFT of the image. Reproduced with permission from D. C. Lee, T. Hanrath and B. A. Korgel, *Angew. Chem., Int. Ed.*, 2005, **44**, 3573. © 2005 Wiley-VCH Verlag GmbH & Co. KGaA

Solution–liquid–solid synthesis of germanium nanowires gives high yields.<sup>171</sup> In this work, Bi nanocrystals were used as seeds for promoting nanowire growth in TOP, by the decomposition of  $\text{GeI}_2$  at 623 K. A solid-phase seeded growth with nickel nanocrystals yields Ge nanowires by the thermal decomposition of diphenylgermane in supercritical toluene.<sup>172</sup> A patterned growth of freestanding single-crystalline Ge nanowires with uniform distribution and vertical projection has been accomplished.<sup>173</sup>

High yields of Ge nanowires and nanowire arrays have been obtained by low-temperature CVD by using patterned gold nanoseeds.<sup>174</sup> Ge nanowires have been synthesized starting from the alkoxide, by using a solution procedure involving the injection of a germanium 2,6-dibutylphenoxide solution in oleylamine into a 1-octadecene solution heated to 573 K under an argon atmosphere.<sup>175</sup>

A simple solution-based procedure has been discovered for the synthesis of nanowires of *t*-Se.<sup>176</sup> In this method, selenium powder is first reacted with NaBH<sub>4</sub> in water to yield NaHSe which being unstable decomposes to give amorphous selenium. The nascent selenium imparts a wine red colour to the aqueous solution. On standing for a few hours, the solution transforms into amorphous Se in colloidal form. A small portion of the dissolved selenium precipitates as *t*-Se nanoparticles which act as nuclei to form the one-dimensional nanowires as seen in Fig. 17. The same reaction carried out under hydrothermal conditions yields nanotubes as shown in Fig. 17e. Extending the above strategy, Te nanorods, nanowires, nanobelts and junction nanostructures have been obtained.<sup>177</sup> Micellar solutions of nonionic surfactants can be employed to prepare nanowires and nanobelts of *t*-Se.<sup>178</sup> Se nanowires have been prepared at room temperature by using ascorbic acid as a reducing agent in the presence of  $\beta$ -cyclodextrin<sup>179</sup> and also generated at liquid–liquid interface between water and *n*-butyl alcohol.<sup>180</sup>

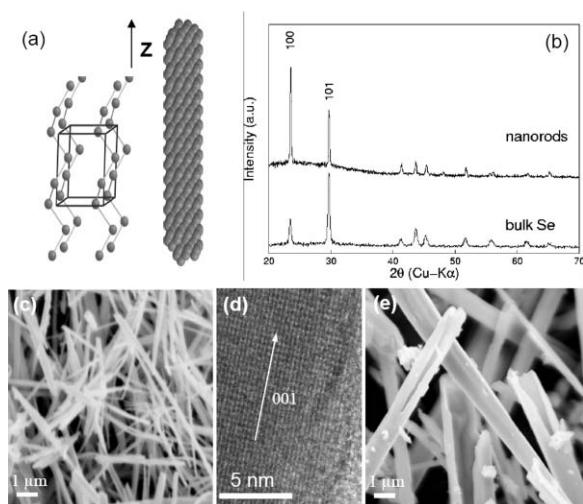


**Fig. 17** (a) Crystal structure of *t*-Se showing a unit cell with helical chains of covalently bonded Se atoms extended along the *c*-axis. The growth direction of the 1D nanostructures is shown along with an atomic model of a rod. (b) XRD patterns of the *t*-Se nanorods and bulk selenium powder used as the starting reagent. (c) SEM image of the Se nanorods obtained after 4 days by reacting 0.025 g of Se with 0.03 g of NaBH<sub>4</sub> in 20 ml water. (d) HREM image of a nanorods (arrow indicates the growth direction of the nanorods). (e) SEM image of *t*-Se scrolls obtained under hydrothermal conditions (From Ref. [176]).

### 4.3 Metal oxides

A seed-assisted chemical reaction at 368 K is found to yield uniform, straight, thin single-crystalline ZnO nanorods on a hectogram scale.<sup>181</sup> Zinc oxide nanowires have been synthesized in large quantities using plasma synthesis.<sup>182</sup> Variable-aspect-ratio,

single crystalline, 1-D nanostructures (nanowires and nanotubes) can be prepared in alcohol/water solutions by reacting Zn<sup>2+</sup> precursor with an organic base, tetraammonium hydroxide.<sup>183</sup> It has been found recently that reaction of water with zinc metal powder or foils at room temperature gives ZnO nanowires.<sup>184</sup> A multi-component precursor has been used to produce nanoparticle nanoribbons of ZnO.<sup>185</sup> Porous ZnO nanoribbons are produced by the self-assembly of textured ZnO nanoparticles. Nanobelts of ZnO can be converted into superlattice-structured nanohelices by a rigid lattice rotation or twisting as seen in Fig. 18.<sup>186</sup> Well-aligned crystalline ZnO nanorods along with nanotubes can be grown from aqueous solutions on Si wafers, poly(ethylene terephthalate) and sapphire.<sup>187</sup> Atomic layer deposition was first used to grow a uniform ZnO film on the substrate of choice and to serve as a templating seed layer for the subsequent growth of nanorods and nanotubes. On this ZnO layer, highly oriented two-dimensional (2-D) ZnO nanorod arrays were obtained by solution growth using Zn(NO<sub>3</sub>)<sub>2</sub> and hexamethylenetetramine in aqueous solution. Controlled growth of aligned ZnO nanorod arrays has been accomplished by an aqueous ammonia solution method.<sup>188</sup> In this method, an aqueous ammonia solution of Zn(NO<sub>3</sub>)<sub>2</sub> is allowed to react with a zinc-coated silicon substrate at a growth temperature of 333–363 K. 3-D interconnected networks of ZnO nanowires

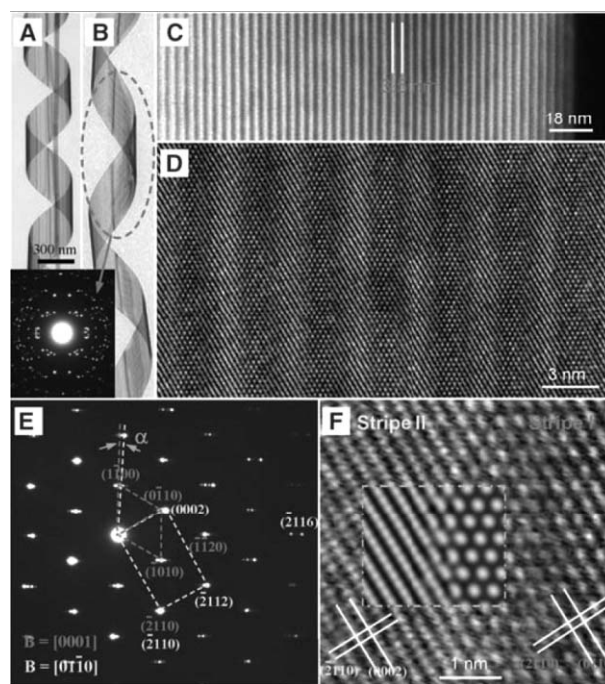


**Fig. 18** (A) Typical low-magnification TEM image of a ZnO nanohelix, showing its structural uniformity. (B) Low-magnification TEM image of a ZnO nanohelix with a larger pitch to diameter ratio. The selected-area ED pattern (SAED, inset) is from a full turn of the helix. (C) Dark-field TEM image from a segment of a nanohelix. The edge at the right and side is the edge of the nanobelt. (D and E) High-magnification TEM image and the corresponding SAED pattern of a ZnO nanohelix with the incident beam perpendicular to the surface of the nanobelt, respectively, showing the lattice structure of the two alternating stripes. (F) Enlarged high-resolution TEM image showing the interface between the two adjacent stripes. From P. X. Gao, Y. Ding, W. Mai, W. L. Hughes, C. Lao and Z. L. Wang, *Science*, 2005, **309**, 1700. Reprinted with permission from AAAS. <http://www.sciencemag.org>

and nanorods have been synthesized by a high temperature solid–vapour deposition process.<sup>189</sup> Templated electrosynthesis of ZnO nanorods wherein, electroreduction of hydrogen peroxide or nitrate ions is carried out to alter the local pH within the pores of the membrane, with the subsequent precipitation of the metal oxide within the pores.<sup>190</sup>

1-D ZnO nanostructures have been synthesized by oxygen assisted thermal evaporation of zinc on a quartz surface over a large area.<sup>191</sup> Pattern- and feature-designed growth of ZnO nanowire arrays for vertical devices has been accomplished by following a pre-designed pattern and feature with controlled site, shape, distribution and orientation.<sup>192</sup>

The ionic liquid 1-*n*-butyl-3-methylimidazolium tetrafluoroborate has been used to synthesize nanoneedles and nanorods of manganese dioxide (MnO<sub>2</sub>).<sup>193</sup> Crystalline silica nanowires were prepared by Deepak *et al.*<sup>194</sup> by a carbothermal procedure. Crystalline SiO<sub>x</sub> nanowires have also been prepared by a low-temperature iron assisted hydrothermal procedure.<sup>195</sup>

IrO<sub>2</sub> nanorods can be grown by metal–organic chemical vapour deposition on sapphire substrates consisting of patterned SiO<sub>2</sub> as the non-growth surface.<sup>196</sup> By employing the hydrothermal route, uniform single-crystalline KNbO<sub>3</sub> nanowires have been obtained.<sup>197</sup>

MgO nanowires and related nanostructures have been produced by carbothermal synthesis, starting with polycrystalline MgO or Mg with or without the use of metal catalysts.<sup>198</sup> This study has been carried out with different sources of carbon, all of them yielding interesting nanostructures such as nanosheets, nanobelts, nanotrees and aligned nanowires. Orthogonally branched single-crystalline MgO nanostructures have been obtained through a simple chemical vapour transport and condensation process in a flowing Ar/O<sub>2</sub> atmosphere.<sup>199</sup>

Ga<sub>2</sub>O<sub>3</sub> powder reacts with activated charcoal, carbon nanotubes or activated carbon around 1373 K in flowing Ar to give nanowires, nanorods and other novel nanostructures of Ga<sub>2</sub>O<sub>3</sub> such as nanobelts and nanosheets.<sup>200</sup> Catalyst-assisted VLS growth of single-crystal Ga<sub>2</sub>O<sub>3</sub> nanobelts has been accomplished by graphite-assisted thermal reduction of a mixture of Ga<sub>2</sub>O<sub>3</sub> and SnO<sub>2</sub> powders under controlled conditions.<sup>201</sup> Zig-zag and helical one-dimensional nanostructures of  $\alpha$ -Ga<sub>2</sub>O<sub>3</sub> have been produced by the thermal evaporation of Ga<sub>2</sub>O<sub>3</sub> in the presence of GaN.<sup>202</sup> Large scale synthesis of TiO<sub>2</sub> nanorods has been achieved by the non-hydrolytic sol–gel ester elimination reaction, wherein the reaction is carried out between titanium(IV) isopropoxide and oleic acid.<sup>203</sup> Single-crystalline and well faceted VO<sub>2</sub> nanowires with rectangular cross sections have been prepared by the vapour transport method, starting with bulk VO<sub>2</sub> powder.<sup>204</sup> Copious quantities of single-crystalline and optically transparent Sn-doped In<sub>2</sub>O<sub>3</sub> (ITO) nanowires have been grown on gold-sputtered Si substrates by carbon-assisted synthesis, starting with a powdered mixture of the metal nitrates or with a citric acid gel formed by the metal nitrates.<sup>205</sup> Vertically aligned and branched ITO nanowire arrays which are single-crystalline have been grown on yttrium-stabilized zirconia substrates containing thin gold films of 10 nm thickness.<sup>206</sup>

Bicrystalline nanowires of hematite ( $\alpha$ -Fe<sub>2</sub>O<sub>3</sub>) have been synthesized by the oxidation of pure Fe.<sup>207</sup> Single-crystalline hexagonal  $\alpha$ -Fe<sub>2</sub>O<sub>3</sub> nanorods and nanobelts can be prepared by a simple iron–water reaction at 673 K.<sup>208</sup> Mesoporous quasi-single crystalline

nanowire arrays of Co<sub>3</sub>O<sub>4</sub> have been grown by immersing Si or fluorine doped SnO<sub>2</sub> substrates in a solution of Co(NO<sub>3</sub>)<sub>2</sub> and concentrated aqueous ammonia.<sup>209</sup> Networks of WO<sub>3-x</sub> nanowires are obtained by the thermal evaporation of W powder in the presence of oxygen.<sup>210</sup> The growth mechanism involves ordered oxygen vacancies (100) and (001) planes which are parallel to the (010) growth direction. A general and highly effective one-pot synthetic protocol for producing one-dimensional nanostructures of transition metal oxides such as W<sub>18</sub>O<sub>49</sub>, TiO<sub>2</sub>, Mn<sub>3</sub>O<sub>4</sub> and V<sub>2</sub>O<sub>5</sub> through a thermally induced crystal growth process starting from mixtures of metal chlorides and surfactants, has been described.<sup>211</sup> Self-coiling nanobelts of Ag<sub>2</sub>V<sub>4</sub>O<sub>11</sub> have been obtained by the hydrothermal reaction between AgNO<sub>3</sub> and V<sub>2</sub>O<sub>5</sub>.<sup>212</sup> Polymer-assisted hydrothermal synthesis of single crystalline tetragonal perovskite PZT (PbZr<sub>0.52</sub>Ti<sub>0.48</sub>O<sub>3</sub>) nanowires has been carried out.<sup>213</sup> Nanowires of the type II superconductor YBa<sub>2</sub>Cu<sub>4</sub>O<sub>8</sub> have been synthesized by a biomimetic procedure.<sup>214</sup> The nanowires produced by the calcination of a gel containing the biopolymer chitosan and Y, Ba and Cu salts have mean diameters of 50 ± 5 nm with lengths up to 1 μm. Nanorods of V<sub>2</sub>O<sub>5</sub> prepared by the polyol process self-assemble into microspheres.<sup>215</sup>

#### 4.4 Metal chalcogenides

ZnS nanowires and nanoribbons with wurtzite structure can be prepared by the thermal evaporation of ZnS powder onto silicon substrates, sputter-coated with a thin (~25 Å) layer of Au film.<sup>216</sup> Thermal evaporation of a mixture of ZnSe and activated carbon powders in the presence of a tin-oxide based catalyst yields tetrapod-branched ZnSe nanorod architectures.<sup>217</sup> 1-D nanostructures of CdS have been formed on Si substrates by a thermal evaporation route.<sup>218</sup> The shapes of the 1-D CdS nanoforms were controlled by varying the experimental parameters such as temperature and position of the substrates. Nanorods of luminescent cubic CdS are obtained by injecting solutions of anhydrous cadmium acetate and sulfur in octylamine into hexadecylamine.<sup>219</sup> CdSe nanowires have been produced by the cation-exchange route.<sup>220</sup> By employing the cation-exchange reaction between Ag<sup>2+</sup> and Cd<sup>2+</sup>, Ag<sub>2</sub>Se nanowires are transformed into single-crystal CdSe nanowires. A single-source molecular precursor has been used to obtain blue-emitting, cubic CdSe nanorods (~2.5 nm diameter and 12 nm length) at low temperatures.<sup>221</sup> Thin aligned nanorods and nanowires of ZnS, ZnSe, CdS and CdSe can be produced by using microwave-assisted methodology by starting from appropriate precursors.<sup>222</sup> An organometallic preparation of CdTe nanowires with high aspect ratios in the wurtzite structure has been described.<sup>223</sup> Thermal decomposition of copper-diethyldithiocarbamate (CuS<sub>2</sub>CNEt<sub>2</sub>) in a mixed binary surfactant solvent of dodecanethiol and oleic acid at 433 K gives rise to single-crystalline high aspect ratio ultrathin nanowires of hexagonal Cu<sub>2</sub>S.<sup>224</sup> CdX(X = S, Se) nanorods have been synthesized in ionic liquids in the presence of ethylenediamine (Fig. 9b).<sup>87</sup> ZnSe nanorods can also be prepared by the decomposition of zinc acetate in the presence of dimethylselenourea in [BMIM][MeSO<sub>4</sub>] ionic liquid.

Atmospheric pressure CVD can be employed to prepare arrays and networks of PbS nanowires.<sup>225</sup> Monodisperse PbTe nanorods of sub-10 nm diameter are obtained by sonoelectrochemical means by starting with a lead salt and TeO<sub>2</sub> along with nitrotriacetic

acid.<sup>226</sup> Taking bismuth citrate and thiourea in DMF, well-segregated, crystalline  $\text{Bi}_2\text{S}_3$  nanorods have been synthesized by a reflux process.<sup>227</sup> Single-crystalline  $\text{Bi}_2\text{S}_3$  nanowires have also been obtained by using lysozyme which controls the morphology and directs the formation of the 1D inorganic material.<sup>228</sup> In this method,  $\text{Bi}(\text{NO}_3)_3 \cdot 5\text{H}_2\text{O}$ , thiourea and lysozyme are reacted together at 433 K under hydrothermal conditions. A solvent-less synthesis of orthorhombic  $\text{Bi}_2\text{S}_3$  nanorods and nanowires with high aspect ratios ( $>100$ ) has been accomplished by the thermal decomposition of bismuth alkylthiolates in air around 500 K in the presence of the capping agent, octanoate.<sup>229</sup> Single-crystalline  $\text{Bi}_2\text{Te}_3$  nanorods have been synthesized by a template free method at 373 K by the addition of thioglycolic acid or L-cysteine to a bismuth chloride solution.<sup>230</sup>  $\text{GeSe}_2$  nanowires have been obtained by the decomposition of organoammonium selenide (See Fig. 19).<sup>231</sup>  $\text{GeTe}$  nanowires are obtained by a VLS process starting with  $\text{GeTe}$  powder using a Au nanoparticle catalyst.<sup>232</sup> Nanowires of copper indium diselenide have been prepared by the reaction of Se powder with  $\text{In}_2\text{Se}_3$  and anhydrous  $\text{CuCl}_2$  under solvothermal conditions.<sup>233</sup>

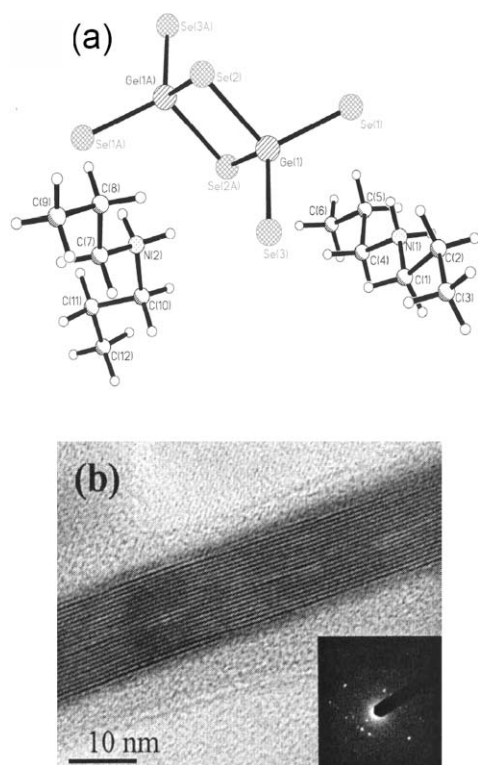


**Fig. 19** (a) Crystal structure of the organoammonium germanium selenide precursor and (b) HREM image of a  $\text{GeSe}_2$  nanowire. The inset shows the typical SAED pattern. (From Ref. [231]).

#### 4.5 Metal pnictides and other nanowires

Single crystalline  $\text{AlN}$ ,  $\text{GaN}$  and  $\text{InN}$  nanowires illustrated in Fig. 20 can be deposited on Si substrates covered with Au islands by using urea complexes formed with the trichlorides of Al, Ga and In as the precursors.<sup>94</sup> Single crystalline  $\text{GaN}$  nanowires are also obtained by the thermal evaporation/decomposition of  $\text{Ga}_2\text{O}_3$  powders with ammonia at 1423 K directly onto a Si substrate coated with a Au film.<sup>234</sup> Direction-dependent homoepitaxial

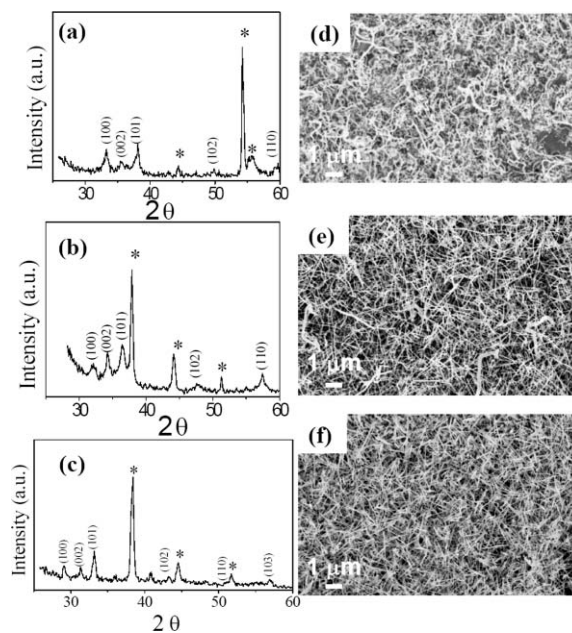


**Fig. 20** XRD patterns of (a)  $\text{AlN}$ , (b)  $\text{GaN}$  and (c)  $\text{InN}$  nanowires respectively (\* indicates peaks arising due to substrate or gold). SEM images of (d)  $\text{AlN}$ , (e)  $\text{GaN}$ , (f)  $\text{InN}$  nanowires. (From Ref. [94]).

growth of  $\text{GaN}$  nanowires has been achieved by controlling the Ga flux during direct nitridation in dissociated ammonia (Fig. 21).<sup>235</sup> The nitridation of Ga droplets at a high flux leads

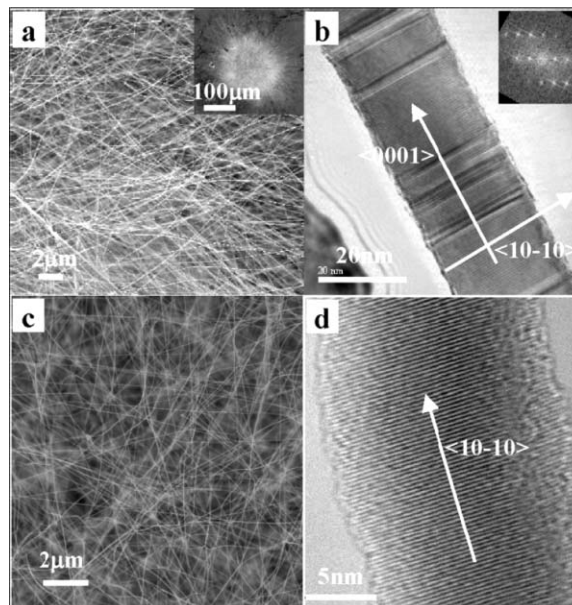


**Fig. 21** (a) SEM images of  $\text{GaN}$  nanowires. The inset shows the spontaneous nucleation and growth of multiple nanowires directly from a larger Ga droplet. (b) HREM image of a  $\text{GaN}$  nanowire. The inset shows FFT of the HREM image, (c) SEM image showing  $\text{GaN}$  nanowires with diameters less than 30 nm resulting from the reactive-vapour transport of a controlled Ga flux in a  $\text{NH}_3$  atmosphere. (d) HREM image of a  $\text{GaN}$  nanowire from the sample shown in (c) indicating that the growth direction is  $\langle 10\text{-}10 \rangle$ . Reproduced with permission from H. Li, A. H. Chin and M. K. Sunkara, *Adv. Mater.*, 2006, **18**, 216. © 2006 Wiley-VCH Verlag GmbH & Co. KGaA

to GaN nanowire growth in the  $c$ -direction ( $\langle 1000 \rangle$ ) as seen in Fig. 21b, while the nitridation with a low Ga flux leads to growth in the  $a$ -direction ( $\langle 10\text{-}10 \rangle$ ) (Fig. 21d). InN nanowires with uniform diameters have been obtained in large quantities by the reaction of  $\text{In}_2\text{O}_3$  powders in ammonia.<sup>236</sup> A general method for the synthesis of Mn-doped nanowires of CdS, ZnS and GaN based on metal nanocluster-catalyzed chemical vapour deposition has been described.<sup>237</sup> Vertically aligned, catalyst-free InP nanowires have been grown on InP(111)B substrates by CVD of trimethylindium and phosphine at 623–723 K.<sup>238</sup>

Nanowires of  $\text{InAs}_{1-x}\text{P}_x$  and  $\text{InAs}_{1-x}\text{P}_x$  heterostructure segments in InAs nanowires, with the P concentration varying from 22% to 100%, have been grown by VLS method.<sup>239</sup> Single-crystalline nanowires of  $\text{LaB}_6$ ,  $\text{CeB}_6$  and  $\text{GdB}_6$  have been deposited on a Si substrate by the reaction of the rare-earth chlorides with  $\text{BCl}_3$  in the presence of hydrogen.<sup>240</sup> Starting from  $\text{BiI}_3$  and  $\text{FeI}_2$ ,  $\text{Fe}_3\text{B}$  nanowires were synthesized on Pt and Pd (Pt/Pd) coated sapphire substrates by CVD at 1073 K.<sup>241</sup> The morphology of the  $\text{Fe}_3\text{B}$  nanowires can be controlled by manipulating the Pt/Pd film thickness and growth time, the typical diameter is in the 5–50 nm range and the length in the 2–30  $\mu\text{m}$  range. Nanowires and nanoribbons of  $\text{NbSe}_3$  have been obtained by the direct reaction of Nb and Se powders.<sup>242</sup> A one-pot metal–organic synthesis of single-crystalline CoP nanowires with uniform diameters has been reported.<sup>243</sup> The method involves the thermal decomposition of cobalt(II) acetylacetonate and tetradecylphosphonic acid in a mixture of TOPO and hexadecylamine.

#### 4.6 Oriented attachment

Oriented attachment of nanocrystals is employed to fabricate one-dimensional as well as complex nanostructures. Thus, nanotubes and nanowires of II–VI semiconductors have been synthesized using surfactants.<sup>244</sup> In Fig. 22, we show TEM image of CdS nanowires and CdSe nanotubes obtained using Triton 100-X as surfactant. Oriented attachment-like growth has been observed in CdS, ZnS and CuS nanorods prepared by using hydrogels as templates.<sup>245</sup> The nanorods or nanotubes of CdS and other materials produced in this manner actually consists of nanocrystals. The synthesis of  $\text{SnO}_2$  nanowires from nanoparticles has been investigated.<sup>246</sup> CdSe nanorods can be formed by redox-assisted asymmetric Ostwald ripening of CdSe dots to rods.<sup>247</sup>

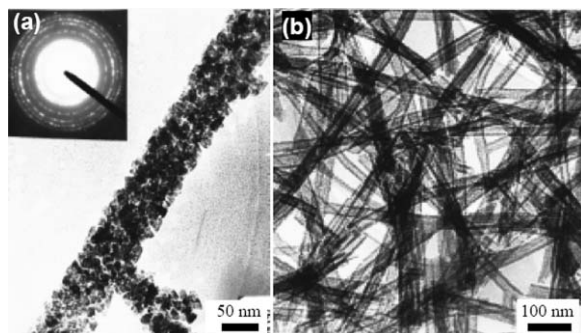


**Fig. 22** TEM images of (a) CdS nanowires (b) CdSe nanotubes obtained by using Triton 100-X as the surfactant. Inset in (a) shows the SAED pattern of the CdS nanowires. Reprinted with permission from C. N. R. Rao, A. Govindaraj, F. L. Deepak, N. A. Gunari and M. Nath, *Appl. Phys. Lett.*, 2001, **78**, 1853. © 2001, American Institute of Physics.

PbSe and cubic ZnS nanowires as well as complex one-dimensional nanostructures can be obtained in solution through oriented attachment of nanocrystals.<sup>248,249</sup> In Fig. 23, star-shaped PbSe nanocrystals and branched nanowires are shown.

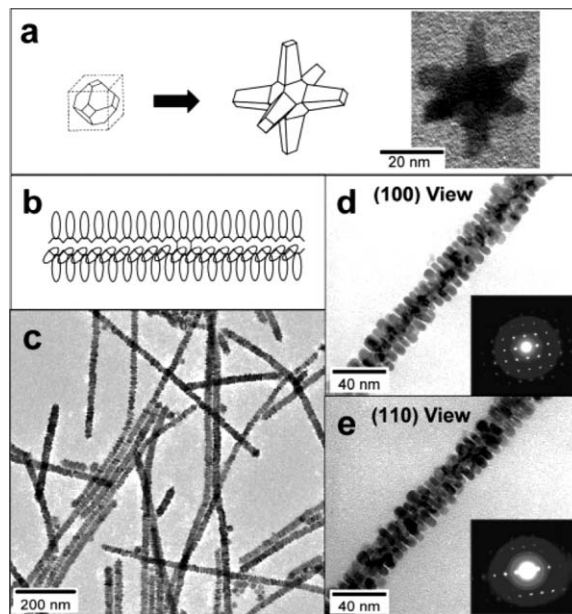


**Fig. 23** (a) Star-shape PbSe nanocrystals and (b–e) radially branched nanowires. (d) TEM image of the (100) view of the branched nanowire and the corresponding selected area electron diffraction pattern. (e) TEM image of the (110) view of the branched nanowire and the corresponding selected area electron diffraction pattern. Reprinted with permission from K.-S. Cho, D. V. Talapin, W. Gaschler and C. B. Murray, *J. Am. Chem. Soc.*, 2005, **127**, 7140. © 2005 American Chemical Society.

#### 4.7 Coaxial cables and other hybrid nanostructures

A general procedure has been proposed for producing chemically bonded ceramic oxide coatings on carbon nanotubes and inorganic nanowires wherein reactive metal chlorides are reacted with acid-treated carbon nanotubes or metal oxide nanowires, followed by hydrolysis with water.<sup>250</sup> On repeating the above process several times followed by calcination, oxide coatings of the desired thickness are obtained. Core-sheath CdS and polyaniline (PANI) coaxial nanocables with enhanced photoluminescence have been fabricated by an electrochemical method using a porous anodic alumina membrane as the template.<sup>251</sup> SiC nanowires can be coated with Ni and Pt nanoparticles ( $\sim 3$  nm) by plasma-enhanced CVD.<sup>252</sup> Single and double-shelled coaxial core-shell nanocables of GaP with  $\text{SiO}_x$  and carbon ( $\text{GaP}/\text{SiO}_x$ ,  $\text{GaP}/\text{C}$ ,  $\text{GaP}/\text{SiO}_x/\text{C}$ ), with selective morphology and structure, have been synthesized by thermal CVD.<sup>253</sup> Silica-sheathed  $3\text{C-Fe}_7\text{S}_8$  has been prepared on silicon substrates with  $\text{FeCl}_2$  and sulfur precursors at 873–1073 K.<sup>254</sup>

Nanowires containing multiple GaP–GaAs junctions are grown by the use of metal–organic vapour phase epitaxy on  $\text{SiO}_2$ .<sup>255</sup> Silica-coated PbS nanowires have been deposited by CVD using  $\text{PbCl}_2$  and S on silicon substrates at temperatures between 650 and 973 K.<sup>256</sup> A novel silica-coating procedure has been devised for CTAB-stabilized gold nanorods and for the hydrophobation of the silica shell with octadecyltrimethoxysilane (OTMS).<sup>257</sup> A

combination of the polyelectrolyte layer-by-layer technique and the hydrolysis followed by condensation of tetraethoxylorthosilicate in a 2-propanol–water mixture leads to homogeneous coatings with control on shell thickness. On the other hand, the strong binding of CTAB molecules to the gold surface makes surface hydrophobation difficult but the functionalization with OTMS, which contains a long hydrophobic hydrocarbon chain, allows the particles to be transferred into nonpolar organic solvents such as chloroform.

Fabrication of InP/InAs/InP core-multishell heterostructure nanowire arrays shown in Fig. 24 has been achieved by selective area metal–organic vapour phase epitaxy.<sup>258</sup> These core–multishell nanowires were designed to accommodate a strained InAs quantum well layer in a higher band gap InP nanowire. Precise control over the nanowire growth direction and the heterojunction formation enabled the successful fabrication of the nanostructure in which all the three layers were epitaxially grown without the assistance of a catalyst.

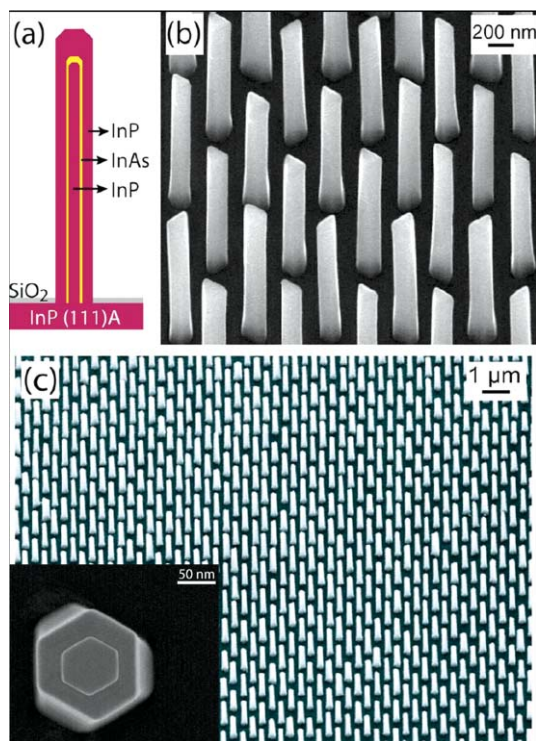


**Fig. 24** (a) Schematic cross-sectional image of InP/InAs/InP core-multishell nanowire. (b) SEM image of periodically aligned InP/InAs/InP core-multishell nanowire array. (c) SEM image showing highly dense ordered arrays of core-multishell nanowires. Schematic illustration and high resolution SEM cross-sectional image of a typical core-multishell nanowire observed after anisotropic dry etching and stain etching. Inset shows the top view of a single nanowire. Reprinted with permission from P. Mohan, J. Motohisa and T. Fukui, *Appl. Phys. Lett.*, 2006, **88**, 133105. © 2006, American Institute of Physics.

## 5. Inorganic nanotubes

There has been considerable interest in the synthesis of fullerenes and nanotubes of inorganic materials.<sup>4,259</sup> These efforts have primarily been focused on layered inorganic compounds such as

metal dichalcogenides (sulfides, selenides, and tellurides), halides (chlorides, bromides, and iodides), oxides and boron nitride, which possess structures comparable to the structure of graphite. Tenne and coworkers<sup>260–261</sup> first recognized that nanosheets of Mo and W dichalcogenides are unstable against folding and closure and that they can form fullerene-like nanoparticles and nanotubes. Nanotubes and fullerene-like nanoparticles of dichalcogenides such as MoS<sub>2</sub>, MoSe<sub>2</sub> and WS<sub>2</sub> have been prepared by processes such as arc-discharge and laser ablation.<sup>262–264</sup> Chemical routes for the synthesis of fullerenes and nanotubes of metal chalcogenides are more versatile and popular. Nanotubes of MoS<sub>2</sub> and WS<sub>2</sub> can be obtained by heating MoO<sub>3</sub>/WO<sub>3</sub> in a reducing atmosphere and then reacted with H<sub>2</sub>S.<sup>265</sup> In the case of metal selenide nanotubes, H<sub>2</sub>Se is used instead of H<sub>2</sub>S.<sup>266</sup> Recognizing that MoS<sub>3</sub> and WS<sub>3</sub> are likely intermediates in the formation of the disulfides, the trisulfides have been directly decomposed in a H<sub>2</sub> atmosphere to obtain the disulfide nanotubes.<sup>267</sup> Similarly, diselenide nanotubes have been obtained by the decomposition of metal triselenides.<sup>268</sup> The trisulfide route provides a general route for the synthesis of the nanotubes of many metal disulfides such as NbS<sub>2</sub> and HfS<sub>2</sub>.<sup>269,270</sup> The decomposition of precursor ammonium salts (NH<sub>4</sub>)<sub>2</sub>MX<sub>4</sub> (X = S, Se; M = Mo, W) also yields nanotubes.<sup>267</sup> The trichalcogenides are intermediates in the decomposition of the ammonium salts.

Bando and co-workers<sup>271</sup> have prepared BN nanotubes by the reaction of MgO, FeO and B in the presence of NH<sub>3</sub> at 1400 °C. Reaction of boric acid or B<sub>2</sub>O<sub>3</sub> with N<sub>2</sub> or NH<sub>3</sub> at high temperatures in the presence of carbon or catalytic metal particles has been employed in the preparation of BN nanotubes.<sup>272</sup> Boron nitride nanotubes can be grown directly on substrates at 873 K by a plasma-enhanced laser-deposition technique.<sup>273</sup> Recently, GaN nanotube brushes have been prepared using amorphous carbon nanotubes templates obtained using AAO membranes.<sup>274</sup>

Large-scale synthesis of Se nanotubes has been carried out in the presence of CTAB.<sup>275</sup> Nanotubes and onions of GaS and GaSe have been generated through laser and thermally induced exfoliation of the bulk powders (see Fig. 25).<sup>276</sup> Single-wall nanotubes of SbPS<sub>4-x</sub>Se<sub>x</sub> (0 < x < 3) with tuneable bandgap have been synthesized.<sup>277</sup> GaP nanotubes with zinc blende structure have been obtained by the VLS growth.<sup>278</sup> Open-ended gold nanotube arrays have been obtained by the electrochemical deposition of Au on to an array of nickel nanorod templates followed by selective removal of the templates.<sup>279</sup> Free-standing, electro-conductive nanotubular sheets of indium tin oxide with different In/Sn ratios have been fabricated by using cellulose as the template.<sup>280</sup> A low-temperature route for synthesizing highly oriented ZnO nanotubes/nanorod arrays has been reported.<sup>281</sup> In this work, a radio frequency magnetron-sputtering technique was used to prepare ZnO-film-coated substrates for subsequent growth of the oriented nanostructures. Controllable syntheses of SiO<sub>2</sub> nanotubes with dome shaped interiors have been prepared by pyrolysis of silanes over Au catalysts.<sup>282</sup> High aspect-ratio, self-organized nanotubes of TiO<sub>2</sub> are obtained by anodization of titanium.<sup>283</sup> These self-organized porous structures consist of pore arrays with a uniform pore diameter of ~100 nm and an average spacing of 150 nm. The pore mouths are open on the top of the layer while on the bottom of the structure the tubes are closed by the presence of an about 50-nm thick barrier of TiO<sub>2</sub>. Electrochemical etching of titanium under potentiostatic

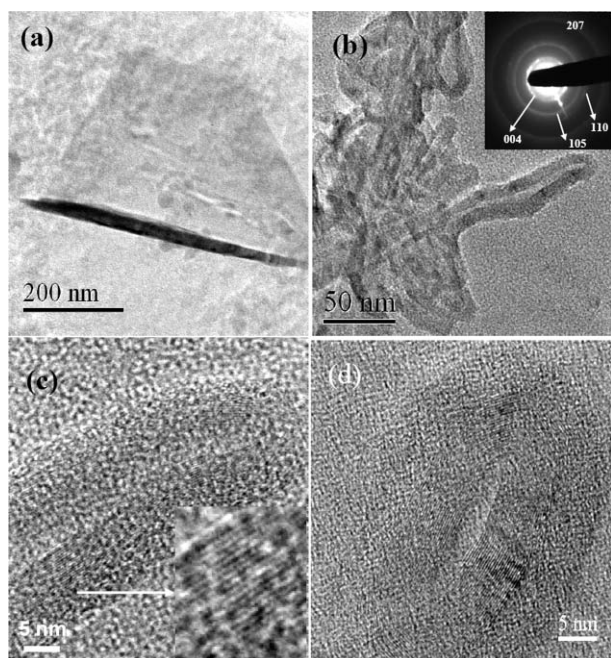


**Fig. 25** TEM images revealing (a) rolling of an exfoliated GaS layer and (b) GaS nanotubes obtained by solvent irradiated laser irradiation. (c) HREM image of a nanotube ( $d = 3.15 \text{ \AA}$ ). Inset shows GaS layer (d) TEM image of a GaSe onion obtained by laser irradiation in *n*-octylamine. Reprinted with permission from U. K. Gautam, S. R. C. Vivekchand, A. Govindaraj, G. U. Kulkarni, N. R. Selvi and C. N. R. Rao, *J. Am. Chem. Soc.*, 2005, **127**, 3658. © 2005, American Chemical Society.

conditions in fluorinated dimethyl sulfoxide and ethanol (1 : 1) under a range of anodizing conditions gives rise to ordered TiO<sub>2</sub> nanotube arrays.<sup>284</sup> TiO<sub>2</sub>-B nanotubes can be prepared by the hydrothermal method.<sup>285</sup> Lithium is readily intercalated into the TiO<sub>2</sub>-B nanotubes up to a composition of Li<sub>0.98</sub>TiO<sub>2</sub> compared with Li<sub>0.91</sub>TiO<sub>2</sub> for the corresponding nanowires. Intercalation of alkali metals into titanate nanotubes has also been investigated.<sup>286</sup> Highly crystalline TiO<sub>2</sub> nanotubes have been synthesized by hydrogen peroxide treatment of low crystalline TiO<sub>2</sub> nanotubes prepared by hydrothermal methods.<sup>287</sup> TiO<sub>2</sub> nanotubes with rutile structure have been prepared by using carbon nanotubes as templates.<sup>288</sup> Anatase nanotubes can be nitrogen doped by ion-beam implantation.<sup>289</sup>

RuO<sub>2</sub> nanotubes have been synthesized by the thermal decomposition of Ru<sub>3</sub>(CO)<sub>12</sub> inside anodic alumina membranes.<sup>290</sup> Transition metal oxide nanotubes have been prepared in water using iced lipid nanotubes as the template.<sup>291</sup> Self-assembled cholesterol derivatives act as a template as well as a catalyst for the sol-gel polymerization of inorganic precursors to give rise to double-walled tubular structures of transition metal oxides.<sup>292</sup> Hydrothermal synthesis of single-crystalline  $\gamma$ -Fe<sub>2</sub>O<sub>3</sub> nanotubes has been accomplished.<sup>293</sup> Nanotubes of single crystalline Fe<sub>3</sub>O<sub>4</sub> have been prepared by wet-etching of the MgO inner cores of MgO/Fe<sub>3</sub>O<sub>4</sub> core-shell nanowires.<sup>294</sup> Cerium oxide nanotubes are prepared by the controlled annealing of the as-formed Ce(OH)<sub>3</sub> nanotubes.<sup>295</sup>

Long hollow inorganic nanoparticle nanotubes with a nanoscale brick wall structure of clay mineral platelets have been

synthesized by templating of block copolymer electrospun fibers with clay mineral platelets followed by interlinking of the platelets using condensation reactions.<sup>296</sup> Similarly, the construction of hollow inorganic nanospheres and nanotubes (inorganic nanostructures) with tunable wall thicknesses (with hollow interiors) is demonstrated by coating on self-assembled polymeric templates (nano-objects) with a thin Al<sub>2</sub>O<sub>3</sub> layer by ALD, followed by removal of the polymer template upon heating.<sup>297</sup> The morphology of the nano-object (*i.e.*, spherical or cylindrical) is controlled by the block lengths of the copolymer. The thickness of the Al<sub>2</sub>O<sub>3</sub> wall is controlled by the number of ALD cycles. Formation of ultra-long single-crystalline ZnAl<sub>2</sub>O<sub>4</sub> spinel nanotubes, through a spinel-forming interfacial solid-state reaction of core-shell ZnO-Al<sub>2</sub>O<sub>3</sub> nanowires involving the Kirkendall effect, has been reported.<sup>298</sup> Polycrystalline lead titanate nano- and microtubes with diameters ranging from a few tens of nanometers up to one micron were fabricated by wetting ordered porous alumina and macroporous silicon with precursor oligomers coupled with templated thermolysis.<sup>299</sup> WC nanotubes can be synthesized by the thermal decomposition of W(CO)<sub>6</sub> in the presence of Mg powder at 1173 K under the autogenic pressure of the precursors in a closed Swagelok reactor.<sup>300</sup>

## 6. Nanocrystalline films generated at the liquid-liquid interface

The liquid-liquid interface has been exploited recently for obtaining ultra-thin nanocrystalline films of a variety of materials. The method involves dissolving an organic precursor of the relevant metal in the organic layer and the appropriate reagent in the aqueous layer. The product formed by the reaction at the interface contains ultra-thin nanocrystalline films of the relevant material formed by closely packed nanocrystals. This simple technique has been shown to yield nanocrystals of metals such as Au, Ag, Pd and Cu, chalcogenides such as CdS, CdSe, ZnS, CoS, NiS, CuS and PbS and oxides such as  $\gamma$ -Fe<sub>2</sub>O<sub>3</sub>, ZnO and CuO.<sup>301-310</sup> In a typical preparation of Au nanocrystalline films, a solution of Au(PPh<sub>3</sub>)Cl in toluene was allowed to stand in contact with aqueous alkali in a beaker at 300 K. Once the two liquid layers were stable, tetrakis(hydroxymethyl)phosphonium chloride (THPC) was injected into the aqueous layer using a syringe with minimal disturbance to the toluene layer.<sup>304</sup> The interface first appears pink, finally growing a robust Au film at the interface. This film could be converted either to a gold organosol or a hydrosol by using appropriate capping agents in the organic and aqueous layers. The thickness and the particle size of the nanocrystals (shown in Fig. 26) is found to be dependent on the reaction conditions employed, such as reactant concentrations, reaction time and temperature.<sup>305</sup> The mean diameters of the nanocrystals formed at 30, 45, 60 and 75 °C are 7, 10, 12 and 15 nm respectively. The liquid-liquid interface has also been employed to prepare nanocrystalline films of binary alloys of Au-Ag and Au-Cu, and also ternary Au-Ag-Cu alloys,<sup>306</sup> by starting with an appropriate mixture of the corresponding metal precursors. Nanocrystalline films of metal chalcogenides such as CdS have been prepared at the toluene-water interface. In a typical preparation of a CdS nanocrystals, Na<sub>2</sub>S was dissolved in water in a beaker and cadmium cupferronate [Cd(cup)<sub>2</sub>], was dissolved in toluene by



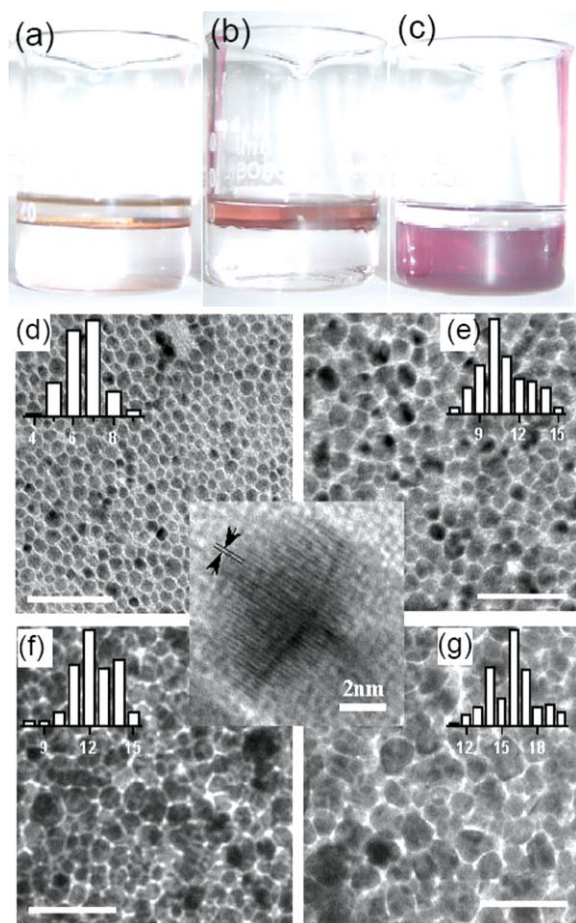


**Fig. 26** (a) Nanocrystalline film of Au formed at the toluene–water interface, (b) When dodecanethiol is added to the toluene layer, the film breaks up, forming an organosol of Au, (c) Au hydrosol obtained when mercaptoundecanoic acid is added to water. TEM images of the ultra-thin nanocrystalline Au films obtained at the liquid–liquid interface after 24 h: (d) 30 °C, (e) 45 °C, (f) 60 °C and (g) 75 °C. The histograms of particle size distribution are shown. The scale bars correspond to 50 nm. A high-resolution image of an individual particle is shown at the center. Reprinted with permission from V. V. Agrawal, G. U. Kulkarni and C. N. R. Rao, *J. Phys. Chem. B*, 2005, **109**, 7300. © 2005, American Chemical Society.

ultrasonication.<sup>307</sup> A few drops of *n*-octylamine were added to the Cd(cup)<sub>2</sub> solution in order to make it completely soluble. The toluene solution was slowly added to a beaker containing the aqueous Na<sub>2</sub>S solution. The interface started appearing yellow within a few minutes and a distinct film was formed after 10 h.  $\gamma$ -Fe<sub>2</sub>O<sub>3</sub> nanocrystals have also been prepared at the toluene–water interface.

While many metals and metal sulfides yield films of nanocrystal assemblies at the liquid–aqueous interface, extended ultra-thin single-crystalline films are obtained in the case of CuS.<sup>308</sup> Single-crystalline films of CuSe, ZnS, PbS, Cu(OH)<sub>2</sub> and ZnO have also been prepared similarly. To prepare a CuS film, 75 mL of 0.12 mM Cu(cup)<sub>2</sub> solution in toluene was slowly added to an aqueous solution of 0.5 mM Na<sub>2</sub>S (75 ml) taken in a crystallization dish (10 cm diameter). An excess of Na<sub>2</sub>S was required in order to prevent the formation of Cu<sub>2</sub>S. The interface gradually turns green, and the CuS film formed at the interface after 12 h, while the two

liquid phases remained colourless. The film grows slowly with time, first appearing as green-islands at the interface (in the initial 1–2 h) and slowly covering the entire interface. The film is fairly continuous and extends over a wide area as can be seen in Fig. 27. Small fragments on the edges of the film are also seen as the film breaks while lifting from the interface (Fig. 27a). The single-crystalline and essentially defect-free nature of the film can be inferred from the HREM image and the SAED pattern (Fig. 27b). The lattice spacing of 2.7 Å in the HREM image corresponds to the separation between (006) planes of the hexagonal CuS phase. The diffraction spots could be indexed on the basis of the hexagonal structure (*P*63/*mmc*, *a* = 3.792 Å and *c* = 16.34 Å). The thickness of the film was estimated to be ~50 nm from AFM and ellipsometric studies. Thicker films could be formed using higher concentration of reactants. The films prepared at higher temperatures are, however, less continuous and form flakes and rods. Nanorods and nanocrystals of various sizes and shapes as seen in Fig. 27d) and Fig. 27e) were obtained upon sonication of the CuS films.

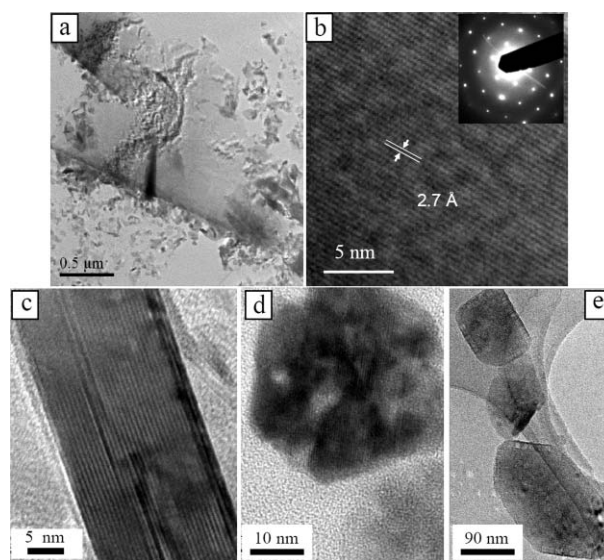


**Fig. 27** (a) TEM images of an ultra-thin 1 μm of CuS obtained at the toluene–water interface. (b) HREM image of the film. Inset shows the corresponding SAED pattern. (c) HREM image of a rod like fragment obtained at 343 K. (d) Hexagonal CuS nanocrystals obtained by sonication of the film obtained with 2 mg of Cu(cup)<sub>2</sub> and (e) the nanocrystals obtained by using 1 mg Cu(cup)<sub>2</sub>. Reprinted with permission from U. K. Gautam, M. Ghosh and C. N. R. Rao, *Langmuir*, 2004, **20**, 10775. © 2004, American Chemical Society.

Extended single-crystalline films of ZnS are obtained by this method starting with Zn(cup)<sub>2</sub> and Na<sub>2</sub>S.<sup>309</sup> The UV-visible absorption spectrum of a ZnS film obtained by reacting 5 mg of Zn(cup)<sub>2</sub> in 50 ml of toluene at ~30 °C for 12 h shows an absorption band at ~320 nm, close to that of bulk ZnS. The PL spectrum of the ZnS film displays a broad emission band centered at ~425 nm due to the presence of sulfur vacancies in the ZnS lattice. A blue-shift of the absorption band to 285 nm was observed when the reaction time was restricted to 1 h, suggesting a thin, incompletely formed film. Unlike chemical methods such as the LB technique, where non-single-crystalline films are obtained by assembling nanocrystals or CVD and related

techniques where stringent conditions as well as substrates are required, the interface method is simple and can be extended to a variety of materials. Using a similar approach CdSe nanofilms have also been prepared.<sup>310</sup>

## 7. Nanowalls

Thermal exfoliation of GaS and GaSe gives rise to nanowalls (Fig. 28). Nanowalls of carbon, which are actually interconnected 2D nanosheets of carbon vertically standing on a substrate has been described by Wu and co-workers.<sup>311</sup> There are reports of ZnO nanowalls and ZnO nanorods grow from the nodes of nanowalls.<sup>312</sup> As mentioned in the previous section, thermal exfoliation of GaSe gave rise to solid deposits in the cooler end of the sealed tube.<sup>313</sup> Deposits with similar morphology were obtained in the case of GaS as well. The deposits contained wall structures with smooth curved surfaces as revealed by the SEM images. The XRD pattern of the sample could be indexed on the hexagonal phase of GaSe. The EDAX spectrum recorded at various locations of the sample confirmed the Ga : Se ratio to be 1 : 1. TEM images revealed that the walls are transparent, especially at the edges, indicating a thickness of around a few nanometers. The nanowalls are single-crystalline, as established by the HREM images as well as the SAED patterns. The lattice spacing observed in the HREM image of 3.229 Å corresponds to the separation between the [100] planes of GaSe in the space group  $P6_3/mmc$ . In the initial stage, the exfoliated sheets deposited in the cooler end of the tube melt forming droplets. Flower-like nanostructures form around these droplets and grow with time forming extended network structures. The Ga<sub>2</sub>O<sub>3</sub> nanowalls were obtained by heating GaS and GaSe nanowalls in air at 823 K. On the other hand, heating the GaS and GaSe nanowalls in NH<sub>3</sub>, GaN nanowalls were obtained.

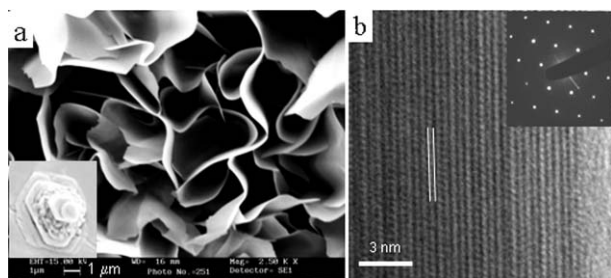


**Fig. 28** (a) SEM image of GaSe nanowalls deposited at 673 K. (b) HREM images of a nanowall. The separation between the lattice planes ( $3.229 \text{ \AA} \approx d_{100}$ ) is shown in the image. Inset shows the SAED pattern. (From Ref. [313]).

## 8. Conclusions

The preceding presentation reflects the tremendous contribution of chemists to the synthesis of inorganic nanomaterials. Beside the use of known methods, the synthesis of nanomaterials has required many newer strategies geared to prepare objects of different dimensionalities. Clearly, there will be continued efforts by a large body of chemists in preparing inorganic nanomaterials, both known and new, by employing novel and improved methods. In addition to synthesis, functionalization, solubilization and assembly of nanomaterials are aspects of great relevance where

again chemistry plays a crucial role. While we have not touched on these aspects in this article, it is necessary that we recognise their importance in the manipulation and use of nanomaterials.

## References

- G. Schmid, Clusters and Colloids, From Theory to Applications, VCH, Weinheim, 1994.
- The Chemistry of Nanomaterials, Ed. C. N. R. Rao, A. Muller and A. K. Cheetham, 2004, Wiley-VCH Verlag, Weinheim, vol. 1 & 2.
- Nanomaterials Chemistry: Recent Developments, Ed. C. N. R. Rao, A. Muller and A. K. Cheetham, 2007, Wiley-VCH-Verlag, Weinheim.
- C. N. R. Rao and A. Govindaraj, Nanotubes and Nanowires, RSC series on Nanoscience, London, 2005.
- C. N. R. Rao, A. Govindaraj and S. R. C. Vivekchand, *Ann. Rep. Prog. Chem.*, Royal Society of Chemistry: London, 2006, **102**, 20.
- C. N. R. Rao, P. J. Thomas and G. U. Kulkarni, *Nanocrystals: Synthesis, Properties and Applications*, Springer series on material science: 95, 2007.
- (a) C. Burda, X. Chen, R. Narayanan and M. A. El-Sayed, *Chem. Rev.*, 2005, **105**, 1025; (b) M. Rajamathi and R. Seshadri, *Curr. Opin. Solid State Mater. Sci.*, 2002, **6**, 337.
- E. A. Hauser and J. E. Lynn, *Experiments in Colloid Chemistry*, p. 18 (McGraw-Hill: New York 1940).
- (a) J. Turkevich, P. C. Stevenson and J. Hillier, *Spec. Discuss. Faraday Soc.*, 1951, **11**, 55; (b) J. Turkevich, *Gold Bull.*, 1985, **18**, 86.
- D. G. Duff, A. Baiker and P. P. Edwards, *Langmuir*, 1993, **9**, 2301.
- M. Brust, M. Walker, D. Bethell, D. J. Schiffrin and R. Whyman, *J. Chem. Soc., Chem. Commun.*, 1994, 801.
- K. V. Sarathy, G. Raina, R. T. Yadav, G. U. Kulkarni and C. N. R. Rao, *J. Phys. Chem. B*, 1997, **101**, 9876.
- K. V. Sarathy, G. U. Kulkarni and C. N. R. Rao, *Chem. Commun.*, 1997, 537.
- P. J. Thomas, G. U. Kulkarni and C. N. R. Rao, *J. Phys. Chem. B*, 2000, **104**, 8138.
- T. Teranishi and M. Miyake, *Chem. Mater.*, 1998, **10**, 594.
- M. Schulz-Dobrick, K. V. Sarathy and M. Jansen, *J. Am. Chem. Soc.*, 2005, **127**, 12816.
- (a) I. Pastoriza-Santos and L. M. Liz-Marzán, *Langmuir*, 2002, **18**, 2888; (b) I. Pastoriza-Santos and L. M. Liz-Marzán, *Pure Appl. Chem.*, 2000, **72**, 83.
- N. R. Jana and X. Peng, *J. Am. Chem. Soc.*, 2003, **125**, 14280.
- R. Jin, Y. Cao and C. A. Mirkin, *Science*, 2001, **294**, 1901.
- R. Jin, Y. Cao, E. Hao, G. S. Métraux, G. C. Schatz and C. A. Mirkin, *Nature*, 2003, **425**, 487.
- G. S. Métraux and C. A. Mirkin, *Adv. Mater.*, 2005, **17**, 412.
- E. Hao, R. C. Bailey and G. C. Schatz, *Nano Lett.*, 2004, **4**, 327.
- C. H. Kuo and M. H. Huang, *Langmuir*, 2005, **21**, 2012.
- Y. Xiao, B. Shytlahovsky, I. Popov, V. Pavlov and I. Wilner, *Langmuir*, 2005, **21**, 5659.
- M. Zhou, S. Chen and S. Zhao, *J. Phys. Chem. B*, 2006, **110**, 4510.
- B. J. Wiley, Y. Xiong, Z.-Y. Li, Y. Yin and Younan Xia, *Nano Lett.*, 2006, **6**, 765.
- T. Tsukatani and H. Fujihara, *Langmuir*, 2005, **21**, 12093.
- G. S. Fonseca, A. P. Umpierre, P. F. P. Fichtner, S. R. Teixeira and J. Dupont, *Chem.-Eur. J.*, 2003, **9**, 3263.
- H. Itoh, K. Naka and Y. Chujo, *J. Am. Chem. Soc.*, 2004, **126**, 3026.
- O. Margeat, C. Amiens, B. Chaudret, P. Lecante and R. E. Banfield, *Chem. Mater.*, 2005, **17**, 107.
- J. D. Hoefelmeyer, K. Niesz, G. A. Somarjai and T. D. Tilley, *Nano Lett.*, 2005, **5**, 435.
- C. A. Stowell and B. A. Korgel, *Nano Lett.*, 2005, **5**, 1203.
- S. Ghosh, M. Ghosh and C. N. R. Rao, *J. Cluster Sci.*, 2007, **18**, 97.
- O. Margeat, C. Amiens, B. Chaudret, P. Lecante and R. E. Banfield, *Chem. Mater.*, 2005, **17**, 107.
- H. Song, F. Kim, S. Connor, G. A. Samorjai and P. Yang, *J. Phys. Chem. B*, 2005, **109**, 188.
- C. Roychowdhury, F. Matsumoto, P. F. Mutolo, H. A. Abruna and F. J. DiSalvo, *Chem. Mater.*, 2005, **17**, 5871.
- G. De and C. N. R. Rao, *J. Mater. Chem.*, 2005, **15**, 891.
- M. Chen, J. Kim, J. P. Liu, H. Fan and S. Sun, *J. Am. Chem. Soc.*, 2006, **128**, 7132.

- 39 J. Rockenberger, E. C. Scher and A. P. Alivisatos, *J. Am. Chem. Soc.*, 1999, **121**, 11595.
- 40 M. Ghosh, E. V. Sampathkumaran and C. N. R. Rao, *Chem. Mater.*, 2005, **17**, 2348.
- 41 M. Ghosh, K. Biswas, A. Sundaresan and C. N. R. Rao, *J. Mater. Chem.*, 2006, **16**, 106.
- 42 M. Ghosh and C. N. R. Rao, *Chem. Phys. Lett.*, 2004, **393**, 493.
- 43 M. Ghosh, R. Seshadri and C. N. R. Rao, *J. Nanosci. Nanotechnol.*, 2004, **4**, 136.
- 44 S. Thimmaiah, M. Rajamathi, N. Singh, P. Bera, F. C. Meldrum, N. Chandrasekhar and R. Seshadri, *J. Mater. Chem.*, 2001, **11**, 3215.
- 45 K. Biswas and C. N. R. Rao, *J. Phys. Chem. B*, 2006, **110**, 842.
- 46 S. Link and M. A. El-Sayed, *Int. Rev. Phys. Chem.*, 2000, **19**, 409.
- 47 K. Biswas, S. V. Bhat and C. N. R. Rao, *J. Phys. Chem. C*, 2007, **111**, 5689.
- 48 J. Park, K. An, Y. Hwang, J. G. Park, H. J. Noh, J. Y. Kim, J. H. Park, N. M. Hwang and T. Hyeon, *Nat. Mater.*, 2004, **3**, 891.
- 49 W. S. Seo, J. H. Shim, S. J. Oh, E. K. Lee, N. H. Hur and J. T. Park, *J. Am. Chem. Soc.*, 2005, **127**, 6188.
- 50 S-H Choi, E-G Kim, J. Park, K. An, N. Lee, A. C. Kim and T. Hyeon, *J. Phys. Chem. B*, 2005, **109**, 14792.
- 51 Z. Hu, D. J. E. Ramirez, B. E. H. Cervera, G. Oskam and P. C. Searson, *J. Phys. Chem. B*, 2005, **109**, 11209.
- 52 J. Joo, S. G. Kwon, J. H. Yu and T. Hyeon, *Adv. Mater.*, 2005, **17**, 1873.
- 53 L. S. Panchakarla, A. Govindaraj and C. N. R. Rao, *J. Cluster Sci.*, 2007, (in print).
- 54 S. O'Brien, L. Brus and C. B. Murray, *J. Am. Chem. Soc.*, 2001, **123**, 12085.
- 55 H. Wu, Y. Yang and Y. C. Cao, *J. Am. Chem. Soc.*, 2006, **128**, 16522.
- 56 N. Pinna, G. Garweiner, M. Antonietti and M. Niederberger, *J. Am. Chem. Soc.*, 2005, **127**, 5608.
- 57 Q. Liu, W. Lu, A. Ma, J. Tang, J. Lin and J. Fang, *J. Am. Chem. Soc.*, 2005, **127**, 5267.
- 58 J. Tang, F. Redl, Y. Zhu, T. Siegrist, L. E. Brus and M. L. Steigerwald, *Nano Lett.*, 2005, **5**, 543.
- 59 G. Li, L. Li, J. B. Goated and B. F. Woodfield, *J. Am. Chem. Soc.*, 2005, **127**, 8659.
- 60 N. Moumen and M.-P. Pileni, *J. Phys. Chem.*, 1996, **100**, 1867.
- 61 N. Moumen and M.-P. Pileni, *Chem. Mater.*, 1996, **8**, 1128.
- 62 C. B. Murray, D. J. Norris and M. G. Bawendi, *J. Am. Chem. Soc.*, 1993, **115**, 8706–8715.
- 63 J. E. Bowen-Katari, V. L. Colvin and A. P. Alivisatos, *J. Phys. Chem.*, 1994, **98**, 4109.
- 64 U. K. Gautam, M. Rajamathi, F. Meldrum, P. Morgan and R. Seshadri, *Chem. Commun.*, 2001, 629.
- 65 U. K. Gautam, R. Seshadri and C. N. R. Rao, *Chem. Phys. Lett.*, 2003, **375**, 560.
- 66 U. K. Gautam and R. Seshadri, *Mater. Res. Bull.*, 2004, **39**, 669.
- 67 X. Chen and R. Fan, *Chem. Mater.*, 2001, **13**, 802.
- 68 L. Qu and X. Peng, *J. Am. Chem. Soc.*, 2002, **124**, 2049.
- 69 Z. A. Peng and X. Peng, *J. Am. Chem. Soc.*, 2001, **123**, 183.
- 70 Z. A. Peng and X. Peng, *J. Am. Chem. Soc.*, 2002, **124**, 33343.
- 71 L. Qu, Z. A. Peng and X. Peng, *Nano Lett.*, 2001, **1**, 333.
- 72 J. Joo, H. B. Na, T. Yu, J. H. Yu, Y. W. Kim, F. Wu, J. Z. Zhang and T. Hyeon, *J. Am. Chem. Soc.*, 2003, **125**, 11100.
- 73 Y. A. Yang, H. Wu, K. R. Williams and Y. J. Cao, *Angew. Chem., Int. Ed.*, 2005, **44**, 6712.
- 74 J. Jasieniak, C. Bullen, J. V. Embden and P. Mulvaney, *J. Phys. Chem. B*, 2005, **109**, 20665.
- 75 P. D. Cozzoli, L. Manna, M. L. Curri, S. Kudera, C. Giannini, M. Striccoli and A. Agostiano, *Chem. Mater.*, 2005, **17**, 1296.
- 76 J. E. Murphy, M. C. Beard, A. G. Norman, S. P. Ahrenkiel, J. C. Johnson, P. Yu, O. I. Micic, R. J. Ellingson and A. J. Nozik, *J. Am. Chem. Soc.*, 2006, **128**, 3241.
- 77 L. Cademartiri, J. Bertolotti, R. Sopianza, D. S. Wiersma, G. Freymann and G. A. Ozin, *J. Phys. Chem. B*, 2006, **110**, 671.
- 78 L. A. Swafford, L. A. Weigand, M. J. Bowers II, J. R. McBride, J. L. Rapaport, T. L. Watt, S. K. Dixit, L. C. Feldman and S. J. Rosenthal, *J. Am. Chem. Soc.*, 2006, **128**, 12299.
- 79 S.-H. Choi, E.-G. Kim and T. Hyeon, *J. Am. Chem. Soc.*, 2006, **128**, 2520.
- 80 A. Ghezlbash and B. A. Korgel, *Langmuir*, 2005, **21**, 9451.
- 81 See for example: B. Ludolph, M. A. Malik, P. O'Brien and N. Revaprasadu, *Chem. Commun.*, 1998, 1849.
- 82 N. Pradhan and S. Efrima, *J. Am. Chem. Soc.*, 2003, **125**, 2050.
- 83 K. Biswas and C. N. R. Rao, *Chem.–Eur. J.*, 2007, **13**, 6123.
- 84 M. Green, P. Rahman and D. S. Boyle, *Chem. Commun.*, 2007, 574.
- 85 Y. Xie, Y. Qian, W. Wang, S. Zhang and Y. Zhang, *Science*, 1996, **272**, 1926.
- 86 K. Sardar and C. N. R. Rao, *Adv. Mater.*, 2004, **16**, 425.
- 87 (a) U. K. Gautam, K. Sardar, F. L. Deepak and C. N. R. Rao, *Pramana*, 2005, **65**, 549; (b) K. Sardar and C. N. R. Rao, *Solid State Sci.*, 2005, **7**, 217; (c) K. Sardar, F. L. Deepak, A. Govindaraj, M. M. Seikh and C. N. R. Rao, *Small*, 2005, **1**, 91.
- 88 S. V. Bhat, K. Biswas and C. N. R. Rao, *Solid State Commun.*, 2007, **14**, 325.
- 89 K. Biswas, K. Sardar and C. N. R. Rao, *Appl. Phys. Lett.*, 2006, **89**, 132503.
- 90 O. I. Micic, S. P. Ahrenkiel, D. Bertram and A. J. Nozik, *Appl. Phys. Lett.*, 1999, **75**, 478.
- 91 J. L. Coffer, M. A. Johnson, L. Zhang, R. L. Wells and J. F. Janik, *Chem. Mater.*, 1997, **9**, 2671.
- 92 A. C. Frank, F. Stowasser, H. Sussek, H. Pritzkow, C. R. Miskys, O. Ambacher, M. Giersig and R. A. Fischer, *J. Am. Chem. Soc.*, 1998, **120**, 3512.
- 93 A. Manz, A. Brikner, M. Kolbe and R. A. Fischer, *Adv. Mater.*, 2000, **12**, 569.
- 94 K. Sardar, M. Dan, B. Schwenzer and C. N. R. Rao, *J. Mater. Chem.*, 2005, **15**, 2175.
- 95 A. Gomathi and C. N. R. Rao, *Mater. Res. Bull.*, 2006, **41**, 941.
- 96 (a) L. Grocholl, J. Wang and E. G. Gillan, *Chem. Mater.*, 2001, **13**, 4290; (b) L. Grocholl, J. Wang and E. G. Gillan, *Nano Lett.*, 2002, **2**, 899.
- 97 J. Choi and E. G. Gillan, *J. Mater. Chem.*, 2006, **16**, 3774.
- 98 J. Xiao, Y. Xie, R. Tang and W. Luo, *Inorg. Chem.*, 2003, **42**, 107.
- 99 M. Yu, X. Hao, D. Cui, Q. Wang, X. Xu and M. Jiang, *Nanotechnology*, 2003, **14**, 29.
- 100 M. A. Olshavsky, A. B. Goldstein and A. P. Alivisatos, *J. Am. Chem. Soc.*, 1990, **112**, 9438.
- 101 R. L. Wells, S. R. Aubuchon, S. S. Kher and M. S. Lube, *Chem. Mater.*, 1998, **7**, 793.
- 102 O. I. Micic, C. J. Curtis, K. M. Jones, J. R. Sprague and A. J. Nozik, *J. Phys. Chem.*, 1994, **98**, 4966.
- 103 O. I. Micic, J. R. Sprague, C. J. Curtis, K. M. Jones, J. L. Machol, A. J. Nozik, H. Giessen, B. Fluegel, G. Mohs and N. Peyghambarian, *J. Phys. Chem.*, 1995, **99**, 7754.
- 104 A. A. Guzelian, J. E. B. Katari, A. V. Kadavanich, U. Banin, K. Hamad, E. Juban, A. P. Alivisatos, R. H. Wolters, C. C. Arnold and J. R. Heath, *J. Phys. Chem.*, 1996, **100**, 7212.
- 105 S. C. Perera, P. S. Fodor, G. M. Tsoi, L. E. Wenger and S. L. Brock, *Chem. Mater.*, 2003, **15**, 4034.
- 106 S. C. Perera, G. Tsoi, L. E. Wenger and S. L. Brock, *J. Am. Chem. Soc.*, 2003, **125**, 13960.
- 107 S. Wei, J. Lu, W. Yu and Y. Qian, *J. App. Phys.*, 2004, **95**, 3683.
- 108 S. Xu, S. Kumar and T. Nann, *J. Am. Chem. Soc.*, 2006, **128**, 1054.
- 109 M. A. Malik, P. O'Brien and M. Helliwell, *J. Mater. Chem.*, 2005, **15**, 1463.
- 110 K. L. Stamm, J. C. Garno, G. Liu and S. L. Brock, *J. Am. Chem. Soc.*, 2003, **125**, 4038.
- 111 P. Arumugam, S. S. Shinozaki, R. Wang, G. Maob and S. L. Brock, *Chem. Commun.*, 2006, 1121.
- 112 J. Lu, Y. Xie, X. Jiang, W. He and G. Du, *J. Mater. Chem.*, 2001, **11**, 3281.
- 113 W. Schartl, *Adv. Mater.*, 2000, **12**, 1899.
- 114 See for example: X. Peng, M. C. Schlamp, A. V. Kadavanich and A. P. Alivisatos, *J. Am. Chem. Soc.*, 1997, **119**, 7019.
- 115 M. A. Hines and P. Guyot-Sionnest, *J. Phys. Chem.*, 1996, **100**, 468.
- 116 M. A. Malik, P. O'Brien and N. Revaprasadu, *Chem. Mater.*, 2002, **14**, 2004.
- 117 D. Pan, Q. Wang, S. Jiang, X. Ji and L. An, *Adv. Mater.*, 2005, **17**, 176.
- 118 R. Xie, U. Kolb, J. Li, T. Basche and A. Mews, *J. Am. Chem. Soc.*, 2005, **127**, 7480.
- 119 Y. Liu, M. Kim, Y. Wang, Y. A. Wang and X. Peng, *Langmuir*, 2006, **22**, 6341.
- 120 Y.-W. Cao and U. Banin, *J. Am. Chem. Soc.*, 2000, **122**, 9692.
- 121 R. H. Morriss and L. F. Collins, *J. Chem. Phys.*, 1964, **41**, 3357.

- 122 L. Lu, H. Wang, Y. Zhou, S. Xi, H. Zhang, J. Hub and B. Zhaob, *Chem. Commun.*, 2002, 144.
- 123 L. Rivas, S. Sanchez-Cortes, J. V. Garcia-Ramos and G. Morcillo, *Langmuir*, 2000, **16**, 9722.
- 124 K. Mallik, M. Mandal, N. Pradhan and T. Pal, *Nano Lett.*, 2001, **1**, 319.
- 125 Y. W. Cao, R. Jin and C. A. Mirkin, *J. Am. Chem. Soc.*, 2001, **123**, 7961.
- 126 J.-W. Hu, Y. Zhang, J.-F. Li, Z. Liu, B. Ren, S.-G. Sun, Z.-Q. Tian and T. Lian, *Chem. Phys. Lett.*, 2005, **408**, 354.
- 127 J. Rivas, R. D. Sanchez, A. Fondado, A. J. Garcia-Bastida, J. Garcia-Otero, J. Mira, D. Baldomir, A. Gonzhlez, I. Lado, M. A. L. Quintela and S. B. Oseroff, *J. Appl. Phys.*, 1994, **76**, 6564.
- 128 C. T. Seip and C. J. O'Connor, *Nanostruct. Mater.*, 1999, **12**, 183.
- 129 J. Lin, W. Zhou, A. Kumbhar, J. Wiemann, J. Fang, E. E. Carpenter and C. J. O'Connor, *J. Solid State Chem.*, 2001, **159**, 26.
- 130 J. Zhang, M. Post, T. Veres, Z. J. Jakubek, J. Guan, D. Wang, F. Normandin, Y. Deslandes and B. Simard, *J. Phys. Chem. B*, 2006, **110**, 7122.
- 131 L. Wang, J. Luo, Q. Fan, M. Suzuki, I. S. Suzuki, M. H. Engelhard, Y. Lin, N. Kim, J. Q. Wang and C.-J. Zhong, *J. Phys. Chem. B*, 2005, **109**, 21593.
- 132 W. Stober, A. Fink and E. Bohn, *J. Colloid Interface Sci.*, 1968, **26**, 62.
- 133 See for example: M. A. Correa-Duarte, M. Giersig, N. A. Kotov and L. M. Liz-Marzán, *Langmuir*, 1998, **14**, 6430.
- 134 See for example: T. Ung, L. M. Liz-Marzán and P. Mulvaney, *J. Phys. Chem. B*, 1999, **103**, 6770.
- 135 L. M. Liz-Marzán, M. Giersig and P. Mulvaney, *Langmuir*, 1996, **12**, 4329.
- 136 K. S. Mayya, D. I. Gittins and F. Caruso, *Chem. Mater.*, 2001, **13**, 3833.
- 137 I. Pastoriza-Santos, D. S. Koktysh, A. A. Mamedov, M. Giersig, N. A. Kotov and L. M. Liz-Marzán, *Langmuir*, 2000, **16**, 2731.
- 138 V. Eswaranand and T. Pradeep, *J. Mater. Chem.*, 2002, **12**, 2421.
- 139 R. T. Tom, A. S. Nair, N. Singh, M. Aslam, C. L. Nagendra, R. Philip, K. Vijayamohan and T. Pradeep, *Langmuir*, 2003, **19**, 3439.
- 140 S. Ghosh, K. Biswas and C. N. R. Rao, *J. Mater. Chem.*, 2007, **17**, 2412.
- 141 V. Salgueiriño-Maceira and M. A. C. Duarte, *J. Mater. Chem.*, 2006, **16**, 3539.
- 142 O. Masala and R. Seshadri, *J. Am. Chem. Soc.*, 2005, **127**, 9354.
- 143 C. N. R. Rao, F. L. Deepak, G. Gundiah and A. Govindaraj, *Prog. Solid State Chem.*, 2003, **31**, 5.
- 144 Y. Xia, P. Yang, Y. Sun, Y. Wu, B. Mayers, B. Gates, Y. Yin, F. Kim and H. Han, *Adv. Mater.*, 2003, **15**, 353.
- 145 C. R. Martin, *Science*, 1994, **266**, 1961.
- 146 D. Almwlawi, C. Z. Liu and M. Moskovits, *J. Mater. Res.*, 1994, **9**, 1014.
- 147 A. Govindaraj, B. C. Satishkumar, M. Nath and C. N. R. Rao, *Chem. Mater.*, 2000, **12**, 202.
- 148 M. Zheng, L. Zhang, X. Zhang, J. Zhang and G. Li, *Chem. Phys. Lett.*, 2001, **334**, 298.
- 149 J. A. Sioss and C. D. Keating, *Nano Lett.*, 2005, **5**, 1779.
- 150 B. D. Busbee, S. O. Obare and C. J. Murphy, *Adv. Mater.*, 2003, **15**, 414.
- 151 L. Gou and C. J. Murphy, *Chem. Mater.*, 2005, **17**, 3668.
- 152 H.-Y. Wu, H.-C. Chu, T.-J. Kuo, C.-L. Kuo and M. L. H. Huang, *Chem. Mater.*, 2005, **17**, 6447.
- 153 A. Gulati, H. Liao and J. H. Hafner, *J. Phys. Chem. B*, 2006, **110**, 22323.
- 154 A. Gole and C. J. Murphy, *Chem. Mater.*, 2005, **17**, 1325–1330.
- 155 B. Basnar, Y. Weizmann, Z. Cheglakov and I. Willner, *Adv. Mater.*, 2006, **18**, 713–718.
- 156 C.-K. Tsung, X. Kou, Q. Shi, J. Zhang, M. H. Yeung, J. Wang and G. D. Stucky, *J. Am. Chem. Soc.*, 2006, **128**, 5352.
- 157 A. J. Mieszawska, G. W. Slawinski and F. P. Zamborini, *J. Am. Chem. Soc.*, 2006, **128**, 5622.
- 158 C. Ni, P. A. Hassan and E. W. Kaler, *Langmuir*, 2005, **21**, 3334.
- 159 Y. Sun, B. Gates, B. Mayers and Y. Xia, *Nano Lett.*, 2002, **2**, 165.
- 160 Y. Chen, B. J. Wiley and Y. Xia, *Langmuir*, 2007, **23**, 4120.
- 161 L. Gou, M. Chipara and J. M. Zaleski, *Chem. Mater.*, 2007, **19**, 1755.
- 162 D. Ung, G. Viau, C. Ricolleau, F. Warmont, P. Gredin and F. Fievet, *Adv. Mater.*, 2005, **17**, 338.
- 163 W. Z. Wong, B. Poudel, Y. Ma and Z. F. Ren, *J. Phys. Chem. B*, 2006, **110**, 25702.
- 164 Y. Xiong, H. Cai, B. J. Wiley, J. Wang, M. J. Kim and Y. Xia, *J. Am. Chem. Soc.*, 2007, **129**, 3665.
- 165 S. R. C. Vivekchand, G. Gundiah, A. Govindaraj and C. N. R. Rao, *Adv. Mater.*, 2004, **16**, 1842.
- 166 S.-M. Liu, M. Kobayashi, S. Sato and K. Kimura, *Chem. Commun.*, 2005, 4690.
- 167 D. C. Lee, T. Hanrath and B. A. Korgel, *Angew. Chem., Int. Ed.*, 2005, **44**, 3573.
- 168 A. I. Hochbaum, R. Fan, R. He and P. Yang, *Nano Lett.*, 2005, **5**, 457.
- 169 T. Shimizu, T. Xie, J. Nishikawa, S. Shingubara, S. Senz and U. Gosele, *Adv. Mater.*, 2007, **19**, 917.
- 170 S. Kodambaka, J. B. Hannon, R. M. Tromp and F. M. Ross, *Nano Lett.*, 2006, **6**, 1296.
- 171 X. Lu, D. D. Fanfair, K. P. Johnston and B. A. Korgel, *J. Am. Chem. Soc.*, 2005, **127**, 15718.
- 172 H.-Y. Tuan, D. C. Lee, T. Hanrath and B. A. Korgel, *Chem. Mater.*, 2005, **17**, 5705.
- 173 P. Nguyen, H. T. Ng and M. Meyyappan, *Adv. Mater.*, 2005, **17**, 549.
- 174 D. Wang, R. Tu, L. Zhang and H. Dai, *Angew. Chem., Int. Ed.*, 2005, **44**, 2925.
- 175 H. Gerung, T. J. Boyle, L. J. Tribby, S. D. Bunge, C. J. Brinker and S. M. Han, *J. Am. Chem. Soc.*, 2006, **128**, 5244.
- 176 U. K. Gautam, M. Nath and C. N. R. Rao, *J. Mater. Chem.*, 2003, **13**, 2845.
- 177 U. K. Gautam and C. N. R. Rao, *J. Mater. Chem.*, 2004, **14**, 2530.
- 178 Y. Ma, L. Qi, W. Shen and J. Ma, *Langmuir*, 2005, **21**, 6161.
- 179 Q. Li and V. W.-W. Yam, *Chem. Commun.*, 2006, 1006.
- 180 J. M. Song, J. H. Zhu and S. H. Yu, *J. Phys. Chem. B*, 2006, **110**, 23790.
- 181 H. Zhang, D. Yang, X. Ma, N. Du, J. Wu and D. Gue, *J. Phys. Chem. B*, 2006, **110**, 827.
- 182 B. Cheng, W. Shi, J. M. R-Tanner, L. Zhang and E. T. Samulski, *Inorg. Chem.*, 2006, **45**, 1208.
- 183 H. Peng, Y. Fangli, B. Liuyang, L. Jinlin and C. Yunfa, *J. Phys. Chem. C*, 2007, **111**, 194.
- 184 L. S. Panchakarla, M. A. Shah, A. Govindaraj and C. N. R. Rao, *unpublished results*.
- 185 Z.-Gui, J. Liu, Z. Wang, L. Song, Y. Hu, W. Fan and D. Chen, *J. Phys. Chem. B*, 2005, **109**, 1113.
- 186 P. X. Gao, Y. Ding, W. Mai, W. L. Hughes, C. Lao and Z. L. Wang, *Science*, 2005, **309**, 1700.
- 187 Q. Li, V. Kumar, Y. Li, H. Zhang, T. J. Marks and R. P. H. Chang, *Chem. Mater.*, 2005, **17**, 1001.
- 188 Y. Tak and K. Yong, *J. Phys. Chem. B*, 2005, **109**, 19263.
- 189 P. X. Gao, C. S. Lao, W. L. Hughes and Z. L. Wang, *Chem. Phys. Lett.*, 2005, **408**, 174.
- 190 M. Lai and D. J. Riley, *Chem. Mater.*, 2006, **18**, 2233.
- 191 S. Kar, B. N. Pal, S. Chaudhuri and D. Chakravorty, *J. Phys. Chem. B*, 2006, **110**, 4605.
- 192 J. H. He, J. H. Hsu, C. W. Wang, H. N. Lin, L. J. Chen and Z. L. Wang, *J. Phys. Chem. B*, 2006, **110**, 50.
- 193 L.-X. Yang, Y.-J. Zhu, W.-W. Wang, H. Tong and M.-L. Ruan, *J. Phys. Chem. B*, 2006, **110**, 6609.
- 194 F. L. Deepak, G. Gundiah, Md. M. Shiekh, A. Govindaraj and C. N. R. Rao, *J. Mater. Res.*, 2004, **19**, 2216.
- 195 P. Chen, S. Xie, N. Ren, Y. Zhang, A. Dong, Y. Chen and Y. Tang, *J. Am. Chem. Soc.*, 2006, **128**, 1470.
- 196 G. Wang, D.-S. Tsai, Y.-S. Huang, A. Korotcov, W.-C. Yeh and D. Susanti, *J. Mater. Chem.*, 2006, **16**, 780.
- 197 A. Magrez, E. Vasco, J. W. Seo, C. Dieker, N. Setter and L. Forro, *J. Phys. Chem. B*, 2006, **110**, 58.
- 198 K. P. Kalyanikutty, F. L. Deepak, C. Edem, A. Govindaraj and C. N. R. Rao, *Mater. Res. Bull.*, 2005, **40**, 831.
- 199 Y. Hao, G. Meng, C. Ye, X. Zhang and L. Zhang, *J. Phys. Chem. B*, 2005, **109**, 11204.
- 200 G. Gundiah, A. Govindaraj and C. N. R. Rao, *Chem. Phys. Lett.*, 2002, **351**, 189.
- 201 J. Zhang, F. Jiang, Y. Yang and J. Li, *J. Phys. Chem. B*, 2005, **109**, 13143.
- 202 J. Zhan, Y. Bando, J. Hu, F. Xu and D. Goldberg, *Small*, 2005, **1**, 883.
- 203 J. Joo, S. G. Kwon, T. Yu, M. Cho, J. Lee, J. Yoon and T. Hyeon, *J. Phys. Chem. B*, 2005, **109**, 15297.
- 204 B. S. Guiton, Q. Gu, A. L. Prieto, M. S. Gudiksen and H. Park, *J. Am. Chem. Soc.*, 2005, **127**, 498.

- 205 K. P. Kalyanikutty, G. Gundiah, C. Edem, A. Govindaraj and C. N. R. Rao, *Chem. Phys. Lett.*, 2005, **408**, 389.
- 206 Q. Wan, M. Wei, D. Zhi, J. L. MacManus-Driscoll and M. G. Blamire, *Adv. Mater.*, 2006, **18**, 234.
- 207 R. Wang, Y. Chen, Y. Fu, H. Zhang and C. Kisielowski, *J. Phys. Chem. B*, 2005, **109**, 12245.
- 208 Y. M. Zhao, Y.-H. Li, R. Z. Ma, M. J. Roe, D. G. McCartney and Y. Q. Zhu, *Small*, 2006, **2**, 422.
- 209 Y. Li, B. Tan and Y. Wu, *J. Am. Chem. Soc.*, 2006, **128**, 14258.
- 210 J. Zhou, Y. Ding, S. Z. Deng, L. Gong, N. S. Xu and Z. L. Wang, *Adv. Mater.*, 2005, **17**, 2107.
- 211 J.-W. Seo, Y.-W. Jun, S. J. Ko and J. Cheon, *J. Phys. Chem. B*, 2005, **109**, 5389.
- 212 G. Shen and D. Chen, *J. Am. Chem. Soc.*, 2006, **128**, 11762.
- 213 G. Xu, Z. Ren, P. Du, W. Weng, G. Shen and G. Han, *Adv. Mater.*, 2005, **17**, 907.
- 214 S. R. Hall, *Adv. Mater.*, 2006, **18**, 487.
- 215 A.-M. Cao, J.-S. Hu, H.-P. Liang and L.-J. Wan, *Angew. Chem., Int. Ed.*, 2005, **44**, 4391.
- 216 S. Kar and S. Chaudhuri, *J. Phys. Chem. B*, 2005, **109**, 3298.
- 217 J. Hu, Y. Bando and D. Goldberg, *Small*, 2005, **1**, 95.
- 218 S. Kar and S. Chaudhuri, *J. Phys. Chem. B*, 2006, **110**, 4542.
- 219 P. Christian and P. O'Brien, *Chem. Commun.*, 2005, 2817.
- 220 Y. Jeong, Y. Xia and Y. Yin, *Chem. Phys. Lett.*, 2005, **416**, 246.
- 221 S. G. Thoma, A. Sanchez, P. Provencio, B. L. Abrams and J. P. Wilcoxon, *J. Am. Chem. Soc.*, 2005, **127**, 7611.
- 222 A. B. Panda, G. Glaspell and M. S. El-Shall, *J. Am. Chem. Soc.*, 2006, **128**, 2790.
- 223 S. Kumar, M. Ade and T. Nann, *Chem.–Eur. J.*, 2005, **11**, 2220.
- 224 Z. Liu, D. Xu, J. Liang, J. Shen, S. Zhang and Y. Qian, *J. Phys. Chem. B*, 2005, **109**, 10699.
- 225 J.-P. Ge, J. Wang, H.-X. Zhang, X. Wang, Q. Peng and Y. Li, *Chem.–Eur. J.*, 2005, **11**, 1889.
- 226 X. Giu, Y. Lou, A. C. S. Samia, A. Devadoss, J. D. Burgess, S. Dayal and C. Burda, *Angew. Chem., Int. Ed.*, 2005, **44**, 5855.
- 227 R. Chen, M. H. So, C.-M. Che and H. Sun, *J. Mater. Chem.*, 2005, **15**, 4540.
- 228 F. Gao, Q. Lu and S. Komarneni, *Chem. Commun.*, 2005, 531.
- 229 M. B. Sigman and B. A. Korgel, *Chem. Mater.*, 2005, **17**, 1655.
- 230 A. Purkayastha, F. Lupo, S. Kim, T. Borca-Tasciuc and G. Ramanath, *Adv. Mater.*, 2006, **18**, 496.
- 231 M. Nath, A. Choudhury and C. N. R. Rao, *Chem. Commun.*, 2004, 2698.
- 232 D. Yu, J. Wu, Q. Gu and H. Park, *J. Am. Chem. Soc.*, 2006, **128**, 8148.
- 233 Y. H. Yang and Y. T. Chen, *J. Phys. Chem. B*, 2006, **110**, 17370.
- 234 B. Liu, Y. Bando, C. Tang, F. Xu, J. Hu and D. Goldberg, *J. Phys. Chem. B*, 2005, **109**, 17082.
- 235 H. Li, A. H. Chin and M. K. Sunkara, *Adv. Mater.*, 2006, **18**, 216.
- 236 S. Luo, W. Zhou, Z. Zhang, L. Liu, X. Dou, J. Wang, X. Zhao, D. Liu, Y. Gao, L. Song, Y. Xiang, J. Zhou and S. Xie, *Small*, 2005, **1**, 1004.
- 237 P. V. Radonovic, C. J. Barrelet, S. Gradecak, F. Qian and C. M. Lieber, *Nano Lett.*, 2005, **5**, 1407.
- 238 C. J. Novotny and P. K. L. Yu, *Appl. Phys. Lett.*, 2005, **87**, 203111.
- 239 A. I. Persson, M. T. Björk, S. Jeppesen, J. B. Wagner, L. R. Wallenberg and L. Samuelson, *Nano Lett.*, 2006, **6**, 403.
- 240 H. Zhang, Q. Zhang, G. Zhao, J. Tang, O. Zhou and L.-C. Qin, *J. Am. Chem. Soc.*, 2005, **127**, 13120.
- 241 Y. Li, E. Tevaarwerk and R. P. H. Chang, *Chem. Mater.*, 2006, **18**, 2552.
- 242 Y. S. Hor, Z. L. Xiao, U. Welp, Y. Ito, J. F. Mitchell, R. E. Cook, W. K. Kwok and G. W. Crabtree, *Nano Lett.*, 2005, **5**, 397.
- 243 Y. Li, M. A. Malik and P. O'Brien, *J. Am. Chem. Soc.*, 2005, **127**, 16020.
- 244 C. N. R. Rao, A. Govindaraj, F. L. Deepak, N. A. Gunari and M. Nath, *Appl. Phys. Lett.*, 2001, **78**, 1853.
- 245 K. P. Kalyanikutty, M. Nikhila, U. Maitra and C. N. R. Rao, *Chem. Phys. Lett.*, 2006, **432**, 190.
- 246 E. J. H. Lee, C. Ribeiro, E. Longo and E. R. Leite, *J. Phys. Chem. B*, 2005, **109**, 20842.
- 247 R. Li, Z. Luo and F. Papadimitrakopoulos, *J. Am. Chem. Soc.*, 2006, **128**, 6280–6281.
- 248 K.-S. Cho, D. V. Talapin, W. Gaschler and C. B. Murray, *J. Am. Chem. Soc.*, 2005, **127**, 7140.
- 249 J. H. Yu, J. Joo, H. M. Park, S.-H. Baik, Y. W. Kim, S. C. Kim and T. Hyeon, *J. Am. Chem. Soc.*, 2005, **127**, 5662.
- 250 A. Gomathi, S. R. C. Vivekchand, A. Govindaraj and C. N. R. Rao, *Adv. Mater.*, 2005, **17**, 2757.
- 251 Y. Xi, J. Zhou, H. Guo, C. Cai and Z. Lin, *Chem. Phys. Lett.*, 2005, **412**, 60.
- 252 A. D. LaLonde, M. G. Norton, D. N. McIlroy, D. Zhang, R. Padmanabhan, A. Alkhateeb, H. Man, N. Lane and Z. Holman, *J. Mater. Res.*, 2005, **20**, 549.
- 253 S. Y. Bae, H. W. Seo, H. C. Choi, D. S. Han and J. Park, *J. Phys. Chem. B*, 2005, **109**, 8496.
- 254 H.-X. Zhang, J.-P. Ge, J. Wang, Z. Wang, D.-P. Yu and Y.-D. Li, *J. Phys. Chem. B*, 2005, **109**, 11585.
- 255 M. A. Verheijen, G. Immink, T. de Smet, M. T. Borgström and E. P. A. M. Bakkers, *J. Am. Chem. Soc.*, 2006, **128**, 1353.
- 256 M. Afzaal and P. O'Brien, *J. Mater. Chem.*, 2006, **16**, 1113.
- 257 I. Pastoriza-Santos, J. Pérez-Juste and L. M. Liz-Marzán, *Chem. Mater.*, 2006, **18**, 2465.
- 258 P. Mohan, J. Motohisa and T. Fukui, *Appl. Phys. Lett.*, 2006, **88**, 133105.
- 259 C. N. R. Rao and M. Nath, *Dalton Trans.*, 2003, 1.
- 260 R. Tenne, L. Margulis, M. Genut and G. Hodes, *Nature*, 1992, **360**, 444.
- 261 Y. Feldman, E. Wasserman, D. J. Srolovitch and R. Tenne, *Science*, 1995, **267**, 222.
- 262 M. Chhowalla and G. A. J. Amaratunga, *Nature*, 2000, **407**, 164.
- 263 P. A. Parilla, A. C. Dillon, K. M. Jones, G. Riker, D. L. Schulz, D. S. Ginley and M. J. Heben, *Nature*, 1999, **397**, 114.
- 264 P. A. Parilla, A. C. Dillon, B. A. Parkinson, K. M. Jones, J. Alleman, G. Riker, D. S. Ginley and M. J. Heben, *J. Phys. Chem. B*, 2004, **108**, 6197.
- 265 R. Tenne, *Chem.–Eur. J.*, 2002, **8**, 5296.
- 266 T. Tsirlina, Y. Feldman, M. Homyonfer, J. Sloan, J. L. Hutchison and R. Tenne, *Fullerene Sci. Technol.*, 1998, **6**, 157.
- 267 M. Nath, A. Govindaraj and C. N. R. Rao, *Adv. Mater.*, 2001, **13**, 283.
- 268 M. Nath and C. N. R. Rao, *Chem. Commun.*, 2001, 2336.
- 269 M. Nath and C. N. R. Rao, *J. Am. Chem. Soc.*, 2001, **123**, 4841.
- 270 M. Nath and C. N. R. Rao, *Angew. Chem., Int. Ed.*, 2002, **41**, 3451.
- 271 C. Y. Zhi, Y. Bando, C. Tang and D. Goldbeg, *Solid State Commun.*, 2005, **135**, 67.
- 272 F. L. Deepak, C. P. Vinod, K. Mukhopadhyay, A. Govindaraj and C. N. R. Rao, *Chem. Phys. Lett.*, 2002, **353**, 345.
- 273 J. Wang, V. K. Kayastha, Y. K. Yap, Z. Fan, J. G. Lu, Z. Pan, I. N. Ivanov, A. A. Puzosky and D. B. Geohegan, *Nano Lett.*, 2005, **5**, 2528.
- 274 J. Dinesh, M. Eswaremoorthy and C. N. R. Rao, *J. Phys. Chem. C*, 2007, **111**, 510.
- 275 S.-Y. Zhang, Y. Li, X. Ma and H.-Y. Chen, *J. Phys. Chem. B*, 2006, **110**, 9041.
- 276 U. K. Gautam, S. R. C. Vivekchand, A. Govindaraj, G. U. Kulkarni, N. R. Selvi and C. N. R. Rao, *J. Am. Chem. Soc.*, 2005, **127**, 3658.
- 277 C. D. Malliakas and M. G. Kantzidis, *J. Am. Chem. Soc.*, 2006, **128**, 6538.
- 278 Q. Wu, Z. Hu, C. Liu, X. Wang, Y. Chen and Y. Lu, *J. Phys. Chem. B*, 2005, **109**, 19719.
- 279 M. S. Sander and H. Gao, *J. Am. Chem. Soc.*, 2005, **127**, 12158.
- 280 Y. Aoki, J. Huang and T. Kunitake, *J. Mater. Chem.*, 2006, **16**, 292.
- 281 H. Yu, Z. Zhang, M. Han, X. Hao and F. Zhu, *J. Am. Chem. Soc.*, 2005, **127**, 2378.
- 282 C. Li, Z. Liu, C. Gu, X. Xu and Y. Yang, *Adv. Mater.*, 2006, **18**, 228.
- 283 J. M. Macak, H. Tsuchiya and P. Schumuki, *Angew. Chem., Int. Ed.*, 2005, **44**, 2100.
- 284 C. Ruan, M. Paulose, O. K. Varghese, G. K. Mor and C. A. Grimes, *J. Phys. Chem. B*, 2005, **109**, 15754.
- 285 G. Armstrong, A. R. Armstrong, J. Canales and P. G. Bruce, *Chem. Commun.*, 2005, 2454.
- 286 R. Ma, T. Sasaki and Y. Bando, *Chem. Commun.*, 2005, 948.
- 287 M. A. Khan, H.-T. Jung and O.-B. Yang, *J. Phys. Chem. B*, 2006, **110**, 626.
- 288 D. Eder, I. A. Kinloch and A. H. Windle, *Chem. Commun.*, 2006, 1448.
- 289 A. Ghicov, J. M. Macak, H. Tsuchiya, J. Kunze, V. Haeublein, L. Frey and P. Schmuki, *Nano Lett.*, 2006, **6**, 1080.
- 290 H. Tan, E. Ye and W. Y. Fan, *Adv. Mater.*, 2006, **18**, 619.
- 291 Q. Ji and T. Shimizu, *Chem. Commun.*, 2005, 4411.

- 
- 292 J. H. Jung, T. Shimizu and S. Shinkai, *J. Mater. Chem.*, 2005, **15**, 3979.
- 293 C.-J. Jia, L.-D. Sun, Z.-G. Yan, L.-P. You, F. Luo, X.-D. Han, Y.-C. Pang, Z. Zhang and C. H. Yan, *Angew. Chem., Int. Ed.*, 2005, **44**, 4328.
- 294 Z. Liu, D. Zhang, S. Han, C. Li, B. Lei, W. Lu, J. Fang and C. Zhou, *J. Am. Chem. Soc.*, 2005, **127**, 6.
- 295 C. Tang, Y. Bando, B. Liu and D. Goldberg, *Adv. Mater.*, 2005, **17**, 3005.
- 296 R. H. A. Ras, T. Ruotsalainen, K. Laurikainen, M. B. Linder and O. Ikkala, *Chem. Commun.*, 2007, **13**, 1366.
- 297 R. H. A. Ras, M. Kemell, J. de Wit, M. Ritala, G. ten Brinke, M. Leskela and O. Ikkala, *Adv. Mater.*, 2007, **19**, 102.
- 298 H. J. Fan, M. Knez, R. Scholz, K. Nielsch, E. Pippel, D. Hesse, M. Zacharias and U. Gosele, *Nat. Mater.*, 2006, **5**, 627.
- 299 L. Zhao, M. Steinhart, J. Yu and U. Gosele, *J. Mater. Res.*, 2006, **21**, 685.
- 300 S. V. Pol, V. G. Pol and A. Gedanken, *Adv. Mater.*, 2006, **18**, 2023.
- 301 C. N. R. Rao, G. U. Kulkarni, V. V. Agrawal, U. K. Gautam, M. Ghosh and U. Tumkurkar, *J. Colloid Interface Sci.*, 2005, **289**, 305.
- 302 C. N. R. Rao, G. U. Kulkarni, P. J. Thomas, V. V. Agarwal and P. Saravanan, *Curr. Sci.*, 2003, **85**, 1041.
- 303 Y. Lin, H. Skaff, T. Emrick, A. D. Dinsmore and T. P. Russell, *Science*, 2003, **299**, 226.
- 304 C. N. R. Rao, G. U. Kulkarni, P. J. Thomas, V. V. Agarwal and P. Saravanan, *J. Phys. Chem. B*, 2003, **107**, 7391.
- 305 V. V. Agrawal, G. U. Kulkarni and C. N. R. Rao, *J. Phys. Chem. B*, 2005, **109**, 7300.
- 306 V. V. Agrawal, P. Mahalakshmi, G. U. Kulkarni and C. N. R. Rao, *Langmuir*, 2006, **22**, 1846.
- 307 U. K. Gautam, M. Ghosh and C. N. R. Rao, *Chem. Phys. Lett.*, 2003, **381**, 1.
- 308 U. K. Gautam, M. Ghosh and C. N. R. Rao, *Langmuir*, 2004, **20**, 10775.
- 309 K. P. Kalyanikutty, U. K. Gautam and C. N. R. Rao, *Solid State Sci.*, 2006, **8**, 296.
- 310 K. P. Kalyanikutty, U. K. Gautam and C. N. R. Rao, *J. Nanosci. Nanotechnol.*, 2007, **7**, 1916.
- 311 Y. Wu, B. Yang, B. Zong, H. Sun, Z. Shen and Y. Feng, *J. Mater. Chem.*, 2004, **14**, 469.
- 312 H. T. Nan, J. Li, M. K. Smith, P. Nguyen, A. Cassell, J. Han and M. Meyyappan, *Science*, 2003, **300**, 1249.
- 313 U. K. Gautam, S. R. C. Vivekchand, A. Govindaraj and C. N. R. Rao, *Chem. Commun.*, 2005, 3995.